Optimal Trajectories for Vibration Reduction Based on Exponential Filters

Luigi Biagiotti, Claudio Melchiorri, Lorenzo Moriello

Abstract

In this paper, a new type of trajectories, based on an exponential jerk, is presented along with filters for their online generation. The goal is to generalize constant jerk trajectories, widely used in industrial applications, in order to reduce vibrations of motion systems. As a matter of fact, constant jerk trajectories do not assure a complete vibrations suppression when the damping of the resonant modes is not negligible. The values of the parameters (decay rate and duration) of the jerk impulses that allow residual vibration cancellation are derived in an analytical way as a function of the dynamic characteristics of the plant. Comparisons with the well-known input shaping techniques and with system-inversion-based filters show the advantages of the proposed method in terms of robustness with respect to modelling errors, smoothness of the resulting trajectory, time-duration of the motion under velocity and acceleration constraints.

Index Terms

Trajectory planning, residual vibration, dynamic filters, input shaping, multi-segment trajectory, exponential jerk.

I. Introduction

In many industrial applications, the reduction of machine vibrations may be a relevant issue, as lighter structures and faster motions are always required. For this purpose, a number of different approaches, based on feedback and feedforward techniques, can be applied, [6]. However, the most suitable method for machines, which are usually based on standard control architectures, consists of a proper design (or filtering) of the reference input, which does not require changes in the control scheme or additional sensors. A well-known technique for minimizing the residual vibration in point-to-point motions is represented by input shaping [7], [8], [9], based on a train of impulses of proper amplitude and properly delayed in time which are convoluted with the reference signal. The most common input shapers are the so-called Zero Vibration (ZV) input shaper, which assures in case of perfect knowledge of the parameters of the oscillatory system that no residual vibrations occur and the Zero Vibrations and

L. Biagiotti is with the Department of Engineering “Enzo Ferrari”, University of Modena and Reggio Emilia, Strada Vignolese 905, 41125 Modena, Italy, e-mail: luigi.biagiotti@unimore.it.

C. Melchiorri and L. Moriello are with the Department of Electrical, Electronic and Information Engineering “Guglielmo Marconi”, University of Bologna, Viale Risorgimento 2, 40136 Bologna, Italy, e-mail: {claudio.melchiorri, lorenzo.moriello}@unibo.it.

zero Derivative (ZVD) input shaper, which combines complete vibration suppression with higher robustness with respect to modelling errors. Input shapers have been successfully used in a number of practical applications, such as reduction of crane oscillations, [10], control of industrial machines like XY stages, [11], vibration suppression in flexible robotic arms, [12].

Alternative approaches for vibrations reduction by means of reference signal filtering are based on lowpass and notch filters, expressed either as finite or infinite impulse response filters, but it is worth noticing that they do not guarantee complete vibration cancellation [6]. A technique that assures residual vibrations suppression exploiting the dynamic inversion of the flexible plant has been proposed in [13].

More recently, methods for vibration reduction directly based on a proper definition of the reference signal have been presented, see [14], [15], [16]. These techniques rely on the limitation of jerk impulses, whose duration must be carefully chosen on the basis of the dynamics characteristics of the resonant system. Constant jerk trajectories are the simplest example of this approach, but they assure complete vibration cancellation only in case of totally undumped plants. An improvement has been presented in [16], where asymmetric jerk profiles are used to take into account the damping coefficient of the flexible system. This approach, which is generalized and improved in the present paper, will be discussed in Sec. II.

The paper is organized as follows. After a general overview on limited jerk trajectories, filters for their generation and vibration reduction are presented in Sec. II. The novel filter that provides exponential jerk motion profiles is illustrated in Sec. III, where the values of the parameters that guarantee the residual vibration suppression are derived analytically. Then, in Sec. IV the features of the proposed approach are compared with those of alternative methods for vibration cancellation. The results of experimental tests, conducted to validate this novel method, are reported in Sec. V. Concluding remarks are provided in Sect VI.

II. Motivations and related works

In order to evaluate the features and the effects of the proposed trajectory generator in vibration suppression, the motion system shown in Fig. 1 has been considered because of its significance in the industrial field, where a number of applications can be modeled in this way: a properly controlled electric motor is used to actuate an inertial load, whose moment of inertia is J_l, by means an elastic transmission lightly damped, characterized by an elastic constant k_t and a damping coefficient b_t [1], [2], [3]. By assuming that, because of the control, the actuator behaves like an ideal position source, i.e. $q_m(t) \simeq q_{ref}(t)$, only the mathematical model of the system describing the elastic linkage, which causes vibrations, and the load has been taken into account. It is a SISO (Single Input Single Output) LTI (Linear Time Invariant) system that can be modelled with the transfer function

$$G_{ml}(s) = \frac{Q_l(s)}{Q_m(s)} = \frac{2\delta\omega_n s + \omega_n^2}{s^2 + 2\delta\omega_n s + \omega_n^2} \tag{3}$$

with

$$\omega_n = \sqrt{\frac{k_t}{J_l}}, \qquad \delta = \frac{b_t}{2\sqrt{k_t J_l}}$$

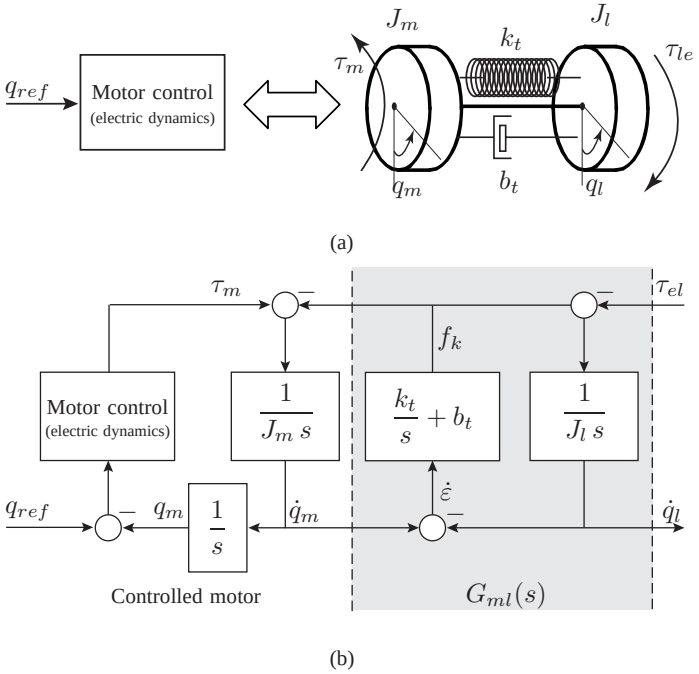

Fig. 1. Lumped constant model of a motion system with elastic linkage (a) and related block-scheme representation (b).

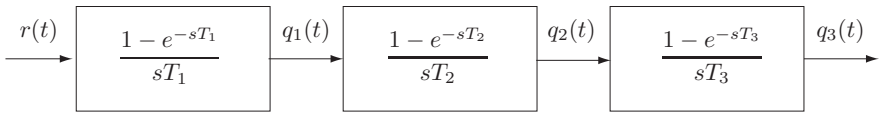

Fig. 2. Structure of a standard third order trajectory generator.

where $Q_m(s) = \mathcal{L}\{q_m(t)\}$ and $Q_l(s) = \mathcal{L}\{q_l(t)\}$ are the Laplace transforms of the motor and load position, respectively. Note that the inertia J_m of the motor has no influence on this model. From (3), it follows that the dynamic relation between the motor position, supposed to be equal to the reference trajectory $q_{ref}(t)$, and the tracking error $\varepsilon(t)$ is

$$\frac{E(s)}{Q_{ref}(s)} = \frac{-s^2}{s^2 + 2\delta\omega_n s + \omega_n^2} \quad \Rightarrow \quad \frac{E(s)}{\ddot{Q}_{ref}(s)} = \frac{-1}{s^2 + 2\delta\omega_n s + \omega_n^2}$$

where $E(s) = \mathcal{L}\{\varepsilon(t)\}$, $Q_{ref}(s) = \mathcal{L}\{q_{ref}(t)\}$ and $\ddot{Q}_{ref}(s) = \mathcal{L}\{\ddot{q}_{ref}(t)\}$. In order to limit residual vibrations, it is therefore necessary that the acceleration profile $\ddot{q}_{ref}(t)$ of the reference trajectory has small spectral components about the resonant frequency of the second order system characterized by (δ, ω_n). In [15] these considerations leaded to a technique for the optimal selection of the parameters of a standard third order trajectory, generated by means of three linear filters

$$M_i(s) = \frac{1 - e^{-sT_i}}{sT_i},$$

as shown in Fig. 2. In particular, parameters

$$T_1 = \frac{|h|}{\mathtt{v}_{max}}, \qquad T_2 = \frac{\mathtt{v}_{max}}{\mathtt{a}_{max}} \tag{4}$$

guarantee that the trajectory from q_0 to q_1 ($h = q_1 - q_0$) complies with the velocity limit $\mathtt{v}_{max}$ and the acceleration limit $\mathtt{a}_{max}$, and the choice

$$T_3 = k\frac{2\pi}{\omega_n} \tag{5}$$

where k is a positive integer number ($k = 1$ is the standard assumption which corresponds to the minimum duration of the period T_3) assures that the spectrum of the trajectory is null for $\omega = \omega_n$ and is therefore able to cancel the residual vibration when the trajectory is applied to an undumped resonant system ($\delta \approx 0$). Unfortunately, if the damping coefficient is not zero, the effectiveness of the filter output (and therefore of standard constant jerk trajectories) in vibration suppression considerably decreases. In Fig. 3 the tracking errors of a resonant system[1] with $\delta = 0.0083$ and $\delta = 0.083$ when a standard third order trajectory is used are compared. Note that if δ grows, when the motion stops (that is for $t \geq T_{tot} = T_1 + T_2 + T_3$), the peak value of the oscillations of the mechanical system accordingly increases. Moreover, also very small values of δ cause vibrations. The effects of damping are analyzed in Fig. 4, where $V\%$, the percent residual vibration[2], is shown as a function of δ. The increasing of vibration's amplitude is consequence of the fact that in the design of the filter $M_3(s)$ the damping coefficient is not considered. The only way to take into account δ is in the selection of the time constant T_3, and therefore in the duration of the constant jerk segment, which can be computed as

$$T_3 = k\frac{2\pi}{\omega_n\sqrt{1-\delta^2}}$$

where, similarly to (5), k is a positive integer number (usually $k = 1$). Unfortunately this choice mitigates but does not solve the problem, as shown in Fig. 4. In order to suppress vibrations in systems whose damping is not negligible, the use of a nonconstant limited jerk profile has been proposed in [16]. In particular, a dynamic filter to be applied to second order trajectories is devised. The filter produces asymmetric jerk segments, characterized by a linear decrease, as shown in Fig. 5. The slope of these segments is computed by solving an optimization problem aiming at minimizing the residual vibration. This approach seems very promising as shown in Fig. 6, where the same conditions of Fig. 3 are considered: in both cases the residual vibrations are completely suppressed.

However, it is worth noticing that some weak points still exist in this technique:

- A closed-form solution for the computation of the filter parameters is not available and the numerical approximation provided in the paper is valid only for δ sufficiently close to 0. For instance, if $\delta = 0.45$ the trajectory does not cancel the residual vibration, as shown in Fig. 7.
- For high values of δ, it may happen that the sign of jerk changes within the same segment. As a consequence the acceleration profiles exhibits undesirable overshoots, see Fig. 5(b).

[1]The numerical values used in [15] are considered.

[2]According to [17], percent residual vibration is defined as the ratio between the residual vibration to a step command with and without shaping filter.

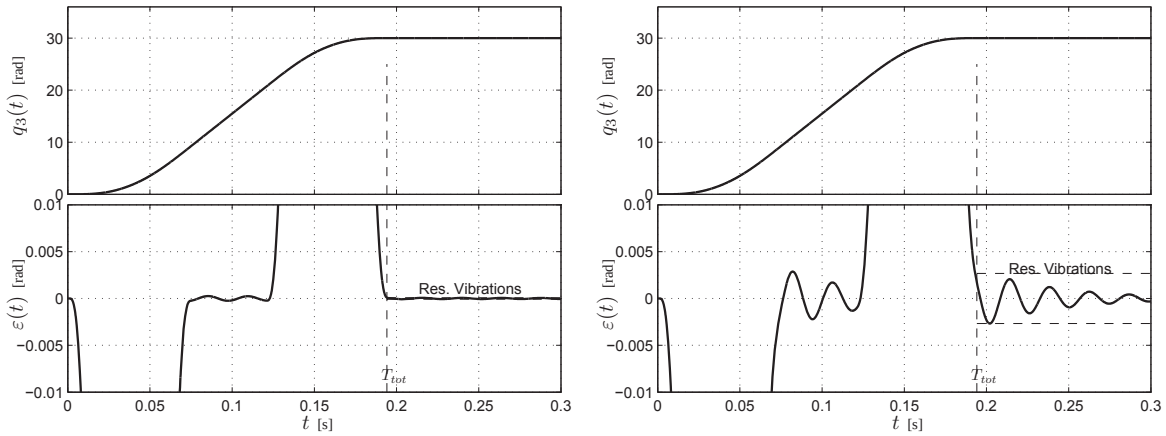

Fig. 3. Residual vibration due to a third order trajectory $q_3(t)$ with $h = 30$ rad, $\mathrm{v}_{max} = 250$ rad/s, $\mathrm{a}_{max} = 5000$ rad/s^2, applied to a second order system with $\omega_n = 260.43$ rad/s and $\delta = 0.0083$ (a) and $\delta = 0.083$ (b).

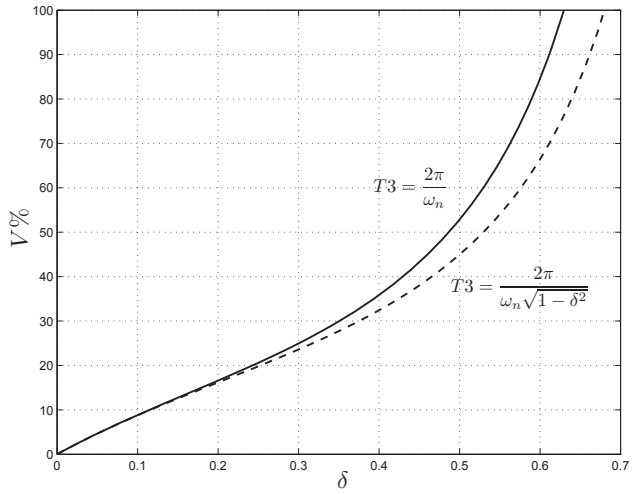

Fig. 4. Percent residual vibration as a function of damping coefficient δ of a second order filter system whose input is filtered by $M_3(s)$.

In order to avoid the above mentioned problems, a shaping technique based on exponential functions is proposed in the next section.

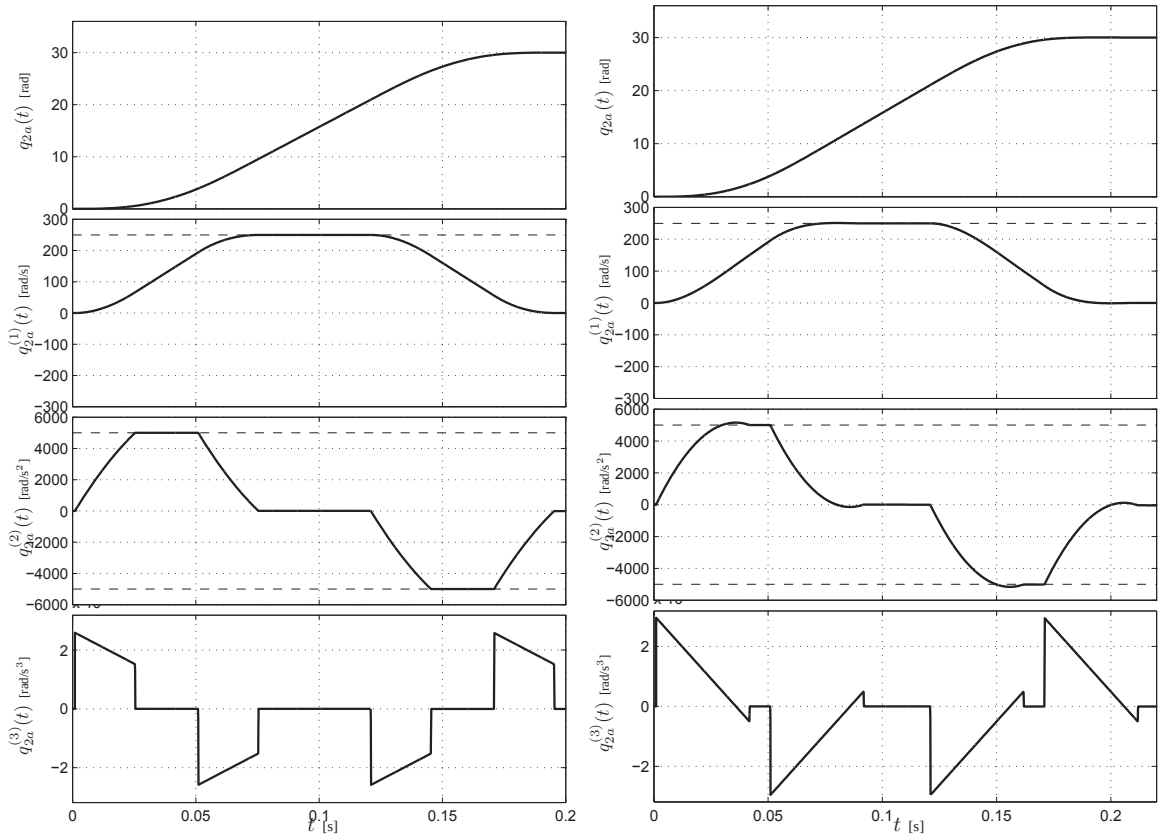

(a) (b)

Fig. 5. Asymmetric jerk trajectory $q_{2,a}$ for $h = 30$ rad, $\mathtt{v}_{max} = 250$ rad/s, $\mathtt{a}_{max} = 5000$ rad/s^2, and $\delta = 0.083$ (a) and $\delta = 0.45$ (b).

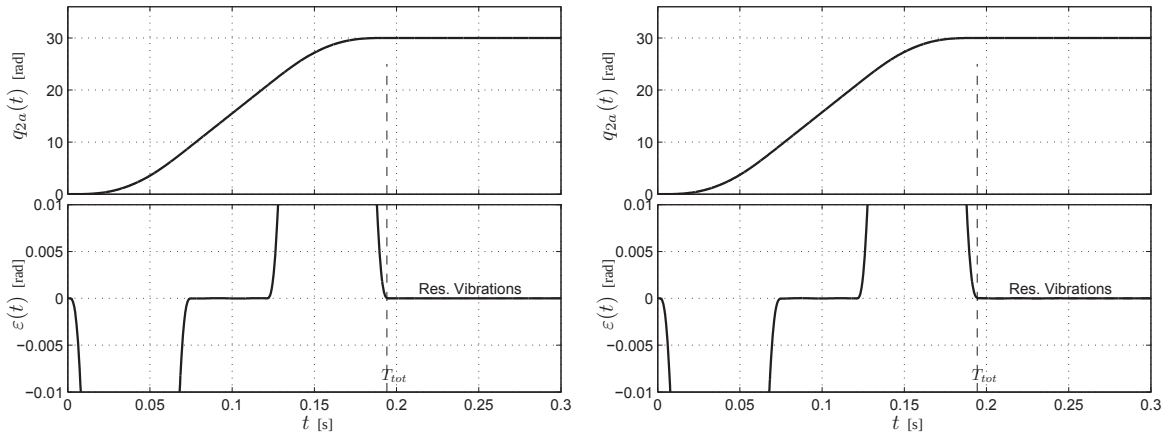

(a) (b)

Fig. 6. Residual vibration due to a third order trajectory with asymmetric jerk $q_{2,a}(t)$ under the same conditions of Fig. 3.

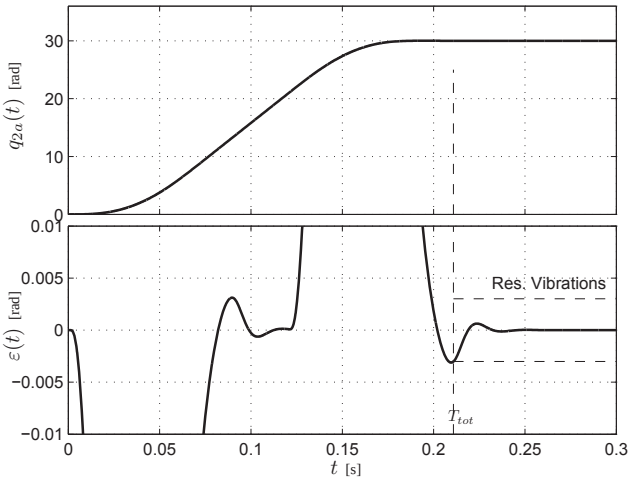

Fig. 7. Residual vibration due to a third order trajectory with asymmetric jerk $q_{2,a}(t)$ when the value $\delta = 0.45$ is considered.

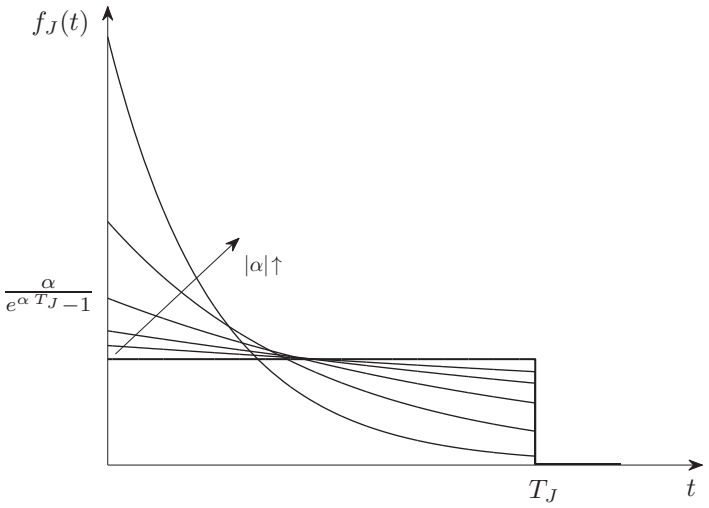

Fig. 8. Impulse response of filter $F_J(s)$ for negative values of parameter α.

III. TRAJECTORIES WITH EXPONENTIAL JERK: DEFINITION AND PROPERTIES

Given a second order trajectory $q_2(t)$, obtained for instance with the cascade of two filters $M_1(s) \cdot M_2(s)$, a multi-segment trajectory with jerk segments defined by exponential functions can be obtained by adding in the chain the filter

$$F_J(s) = \frac{\alpha}{e^{\alpha T_J} - 1} \frac{1 - e^{\alpha T_J} e^{-T_J s}}{s - \alpha} \tag{6}$$

where α and T_j are proper parameters that determine the decay rate and the time duration of impulses composing the jerk profile. As a matter of fact, the impulse response of $F_J(s)$, shown in Fig. 8, is

$$f_J(t) = \frac{\alpha}{e^{\alpha T_J} - 1} e^{\alpha t} \; m(t), \qquad \text{with } m(t) = \begin{cases} 1, & 0 \le t \le T_J \\ 0, & \text{otherwise} \end{cases} .$$

Therefore when applied to the trajectory $q_2(t)$ characterized by a piece-wise constant acceleration, the filter transform the jerk signal composed by impulsive function $\pm \mathtt{a}_{max} \delta(t - t_i)$ in a sequence of exponential segments, see Fig. 9. Note that the maximum value of the jerk can be computed as $\mathtt{j}_{max} = \mathtt{a}_{max} \frac{\alpha}{e^{\alpha T_J} - 1}$.

The filter $F_J(s)$, which does not modify the limit values of velocity and acceleration of the original trajectory $q_2(t)$, can be profitably applied to suppress residual vibrations in those resonant systems that are characterized by significant damping coefficients in lieu of standard third order trajectories with limited, but constant, jerk.

Theorem 1. *The filter $F_J(s)$ in (6) guarantees the complete residual vibration suppression for motion systems with elastic transmission described by (3) fed by step inputs if*

$$\alpha = -\delta \, \omega_n \tag{7}$$

$$T_J = k \frac{2\pi}{\omega_n \sqrt{1 - \delta^2}} \qquad\qquad k = 1, 2, \ldots \tag{8}$$

Proof. When a step input filtered by $F_J(s)$ is applied to the system (3), the tracking error between the load position and the motor position can be computed as

$$E(s) = \frac{-s^2}{s^2 + 2\delta\omega_n s + \omega_n^2} \cdot F_J(s) \cdot \frac{1}{s}. \tag{9}$$

By inverse Laplace transforming $E(s)$ and assuming $t \ge T_J$, the analytic expression of residual vibrations descends:

$$\begin{aligned} \varepsilon(t) = A \Big[& \alpha e^{-\delta\omega_n t} \Big(\cos(\Omega t) - \cos(\Omega(t - T_J)) e^{(\delta\omega_n + \alpha) T_J} \Big) \\ & - B e^{-\delta\omega_n t} \Big(\sin(\Omega t) - \sin(\Omega(t - T_J)) e^{(\delta\omega_n + \alpha) T_J} \Big) \Big] \end{aligned}$$

with $A = \dfrac{\alpha}{(e^{\alpha T_J} - 1)(\alpha^2 + 2\delta\omega_n\alpha + \omega_n^2)}$, $B = \dfrac{\alpha\omega_n\delta + \omega_n^2}{\omega_n\sqrt{1 - \delta^2}}$ and $\Omega = \omega_n\sqrt{1 - \delta^2}$. Therefore, in order to assure that $\varepsilon(t) = 0, \; \forall \; t \ge T_J$ it is sufficient that

$$\begin{aligned} & \delta\omega_n + \alpha = 0 \quad \Leftrightarrow \quad \alpha = -\delta\omega_n \\ & \Omega \, T_J = 2\pi \, k \quad \Leftrightarrow \quad T_J = k \, \frac{2\pi}{\Omega} = k \frac{2\pi}{\omega_n\sqrt{1 - \delta^2}}, \;\; k = 1, 2, \ldots \end{aligned}$$

□

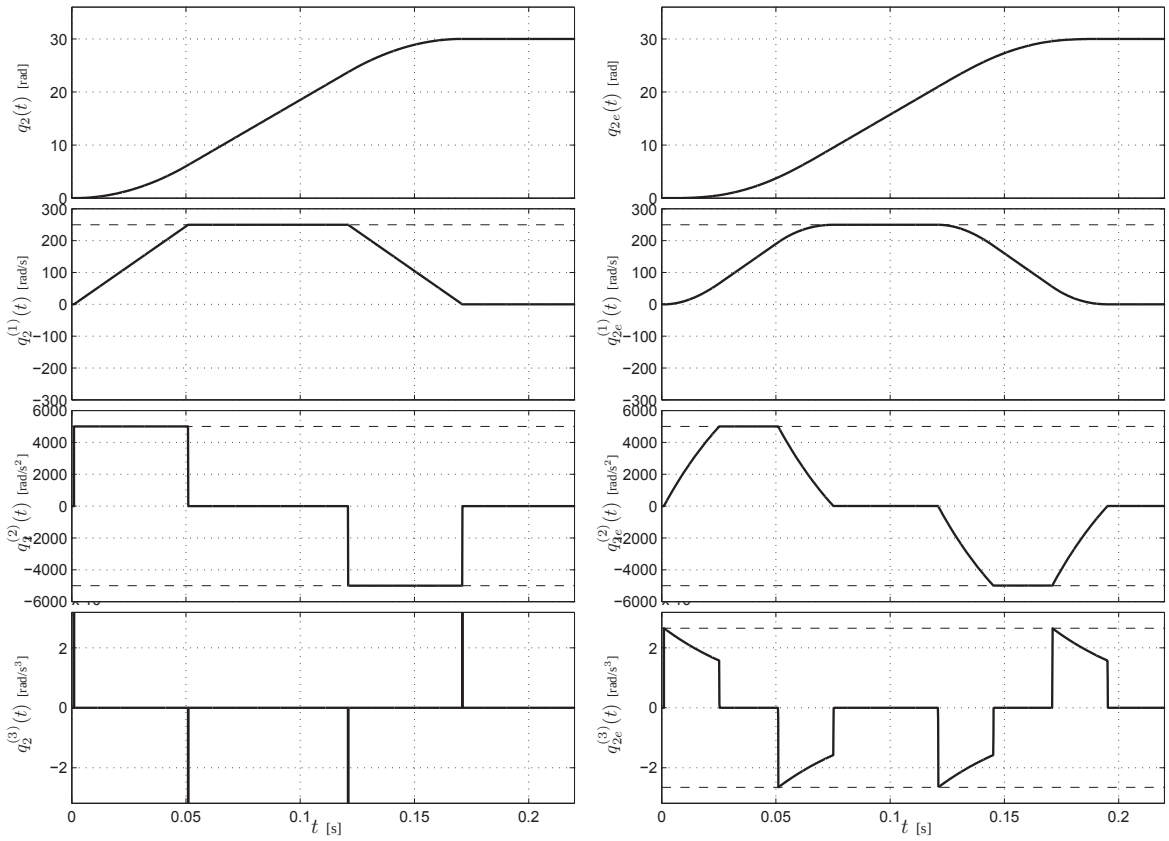

(a) (b)

Fig. 9. Second order trajectory $q_2(t)$ with $h = 30$ rad, $\mathrm{v}_{max} = 250$ rad/s, $\mathrm{a}_{max} = 5000$ rad/s^2, and corresponding exponential jerk trajectory $q_{2,e}$ for $\omega_n = 260.43$ rad/s and $\delta = 0.083$ (b).

Note that $F_J(s)$ is a generalization of a standard filters with rectangular impulse response, which produce piecewise constant jerk profiles. As a matter of fact, when $\delta = 0$ and consequently $\alpha = 0$, the straightforward application of the l'Hôpital's rule leads to

$$\lim_{\alpha \to 0} \frac{\alpha}{e^{\alpha\, T_J} - 1} = \frac{1}{T_J}$$

and therefore

$$\lim_{\delta \to 0} F_J(s) = \lim_{\alpha \to 0} \frac{\alpha}{e^{\alpha\, T_J} - 1} \frac{1 - e^{\alpha\, T_J}\, e^{-T_J\, s}}{s - \alpha} = \frac{1}{T_J} \frac{1 - e^{-sT_J}}{s}.$$

Differently from asymmetric jerk trajectories, the parameters of $F_J(s)$ that assure the complete vibrations cancellations are easily calculable in the whole range of $\delta \in [0, 1[$, and the problems tied to changes in the jerk sign are never present.

Theorem 2. *Third order trajectories with the jerk profile composed by exponential segments satisfying (7) and (8) guarantee that no residual vibrations are present in the resonant system (3).*

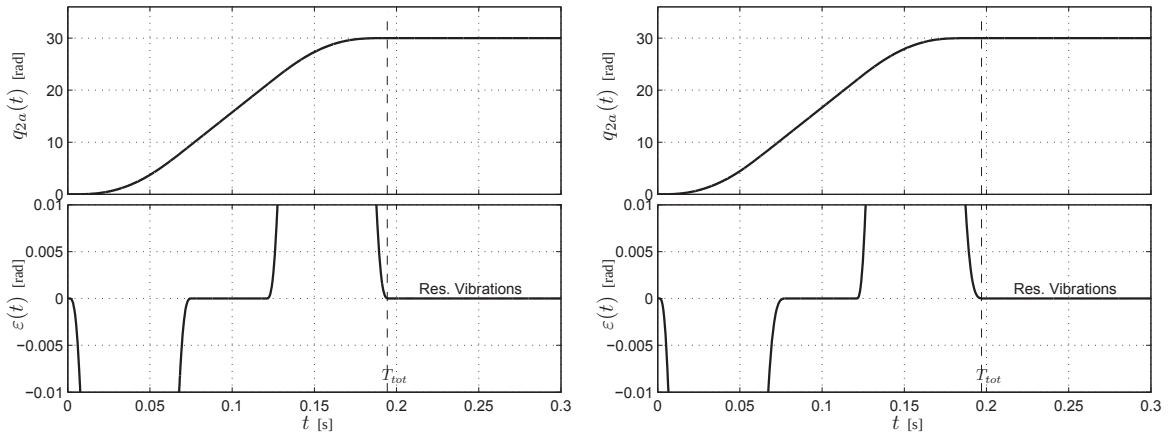

Fig. 10. Residual vibrations due to a third order trajectory with exponential jerk $q_{2,e}(t)$ under the same conditions of Fig. 3, but with $\delta = 0.083$ (a) and $\delta = 0.45$ (b).

Proof. Third order trajectories with exponential jerk, whose analytical expression is reported in Appendix A, can be obtained by filtering a step signal of amplitude h (where h is the desired displacement) with the cascade of linear filters $M_1(s) \cdot M_2(s) \cdot F_J(s)$. Therefore, when the trajectory is applied to the system (3), the tracking error between the load position and the motor position is given by

$$\begin{aligned} E_{q_{2e}}(s) &= \frac{-s^2}{s^2 + 2\delta\omega_n s + \omega_n^2} \cdot \left(M_1(s) \cdot M_2(s) \cdot F_J(s) \cdot \frac{h}{s} \right) \\ &= h \cdot M_1(s) \cdot M_2(s) \cdot \left(\frac{-s^2}{s^2 + 2\delta\omega_n s + \omega_n^2} \cdot F_J(s) \cdot \frac{1}{s} \right) \\ &= h \cdot M_1(s) \cdot M_2(s) \cdot E(s) \end{aligned} \tag{10}$$

where $E_{q_{2e}}(s)$ is the Laplace transform of the tracking error to an exponential jerk trajectory, and $E(s)$ is the transform of the error $\varepsilon(t)$ to a step input, considered in (9). If the conditions (7) and (8) are met, $\varepsilon(t) \neq 0$ only for $t \leq T_J$ and, because the filters $M_1(s)$ and $M_2(s)$ are characterized by a finite length impulse response of duration T_1 and T_2 respectively, from (10) it follows that $\varepsilon_{q_{2e}}(t) \neq 0$ for $t \leq T_1 + T_2 + T_J$ and $\varepsilon_{q_3}(t) = 0$ otherwise. This means that after the end of the reference trajectory (whose duration is $T_{tot} = T_1 + T_2 + T_J$) residual vibrations are completely cancelled. □

In Fig. 10 the tracking errors obtained with exponential jerk trajectories are shown by considering resonant systems with quite different damping coefficients, i.e. $\delta = 0.083$ (a) and $\delta = 0.45$ (b). In both cases residual vibrations are completely suppressed.

A. Parameter identification and sensitivity to errors

The parameters α and T_J which characterize the filter $F_J(s)$ and therefore the trajectory with exponential jerk can be easily determined once the damping coefficient δ and natural frequency ω_n of the system are known.

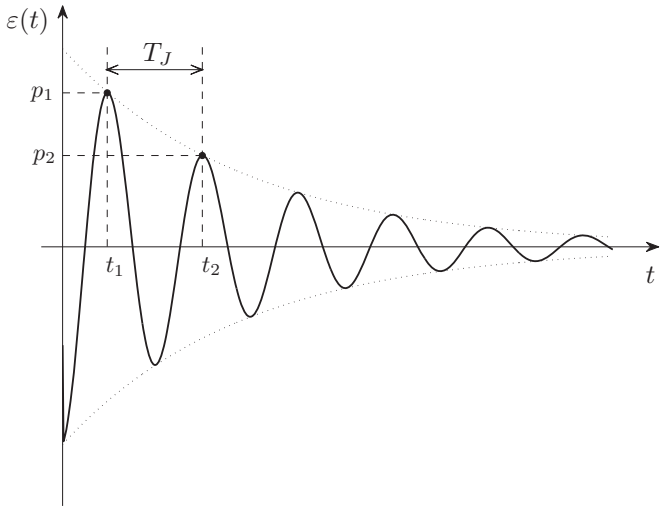

Fig. 11. Residual vibrations caused by the applications of a step input to the system (3).

Alternatively, with standard procedures it is possible to directly deduce their values from the response of the plant to input signals that cause vibrations. For instance, the residual vibrations consequent to a step input are given by

$$\varepsilon_{step}(t) = -\frac{1}{\sqrt{1-\delta^2}} e^{-\delta\omega_n t} \cos\left(\omega_n \sqrt{1-\delta^2}\, t + \varphi_0\right)$$

where $\varphi_0 = \arctan\left(\frac{\delta}{\sqrt{1-\delta^2}}\right)$. Therefore, the ideal values of α and T_J that cancel residual vibrations are respectively the exponential decay constant and the time period of the oscillation. If a measurement of the oscillation is available, it is sufficient to detect two subsequent peak values, as highlighted in Fig. 11, and compute the parameters of the filter as

$$T_J = t_2 - t_1$$
$$\alpha = \frac{1}{T_J} \ln\left(\frac{p_2}{p_1}\right)$$

where the meaning of t_1, t_2, p_1, p_2 is explained in the figure. Note that the period of the oscillation and its decay rate depend on the system, and they do not change also if different type of reference inputs are considered. For instance, second order trajectories, with discontinuous acceleration, can be used in order to provide the actuator with a feasible trajectory and to avoid an excessive strain on the plant. In Fig. 12, the residual vibration caused by a second order trajectory $q_2(t)$ and a step signal applied when $q_2(t)$ stops are compared: it is clear that the only difference is given by the amplitude of the oscillations, which does not influence the procedure for the identification.

Since the identification of the optimal values of the filter parameters does not require an explicit knowledge of the damping coefficient and of the natural frequency of the plant, the robustness of $F_J(s)$ is evaluated by considering errors in σ and T_J with respect to their nominal values, while the sensitivity with respect to changes in δ and ω_n will be analyzed in Sec. IV in order to compare different types of solutions to the problem of the vibrations suppression. In Fig. 13 the percent residual vibration $V\%$ due to errors in the estimation of the parameters α and

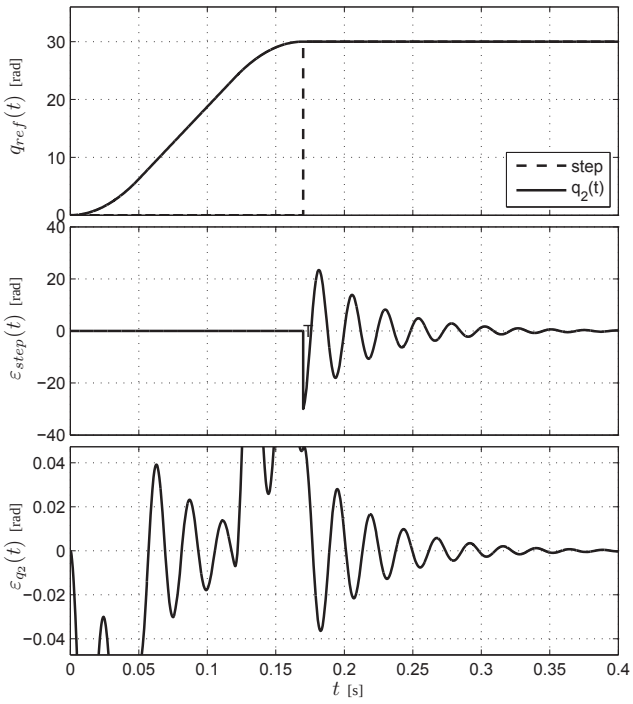

Fig. 12. Comparison between residual vibrations caused by the application of a step input and of a second order trajectory $q_2(t)$ to system (3).

T_J are reported for different values of the damping coefficient and natural frequency of the plant. In particular the ranges $[\hat{\alpha}/2, 2\hat{\alpha}]$ and $[\hat{T}_J/2, 2\hat{T}_J]$ about the nominal values $(\hat{\delta}, \hat{T}_J)$ are considered. From the figure, it is possible to conclude that

- the nominal value of the natural frequency of the plant does not influence the robustness of the filter $F_J(s)$ while the damping coefficient does;
- the choice of T_J is definitely more critical than the choice of α;
- an underestimation of T_J leads to large oscillations; conversely, a value of T_J higher than the nominal one produce limited vibrations especially for high damping coefficients.

B. Sensitivity to unmodeled dynamics of the plant

According to theorem 1 the filter $F_J(s)$ in (6) and consequently the exponential-jerk trajectory obtained when the filter is applied to a second order trajectory $q_2(t)$, like in Fig. 9, guarantee a complete cancellation of the vibrations if the plant can be modelled as a second order system such as (3). However, as already noted in Sec. II typical industrial plants include additional dynamics that may modify the effects of the proposed filter. If the model of the plant includes an additional stable dynamics $\Delta G(s)$, e.g.

$$G(s) = G_{ml}(s)\,\Delta G(s), \tag{11}$$

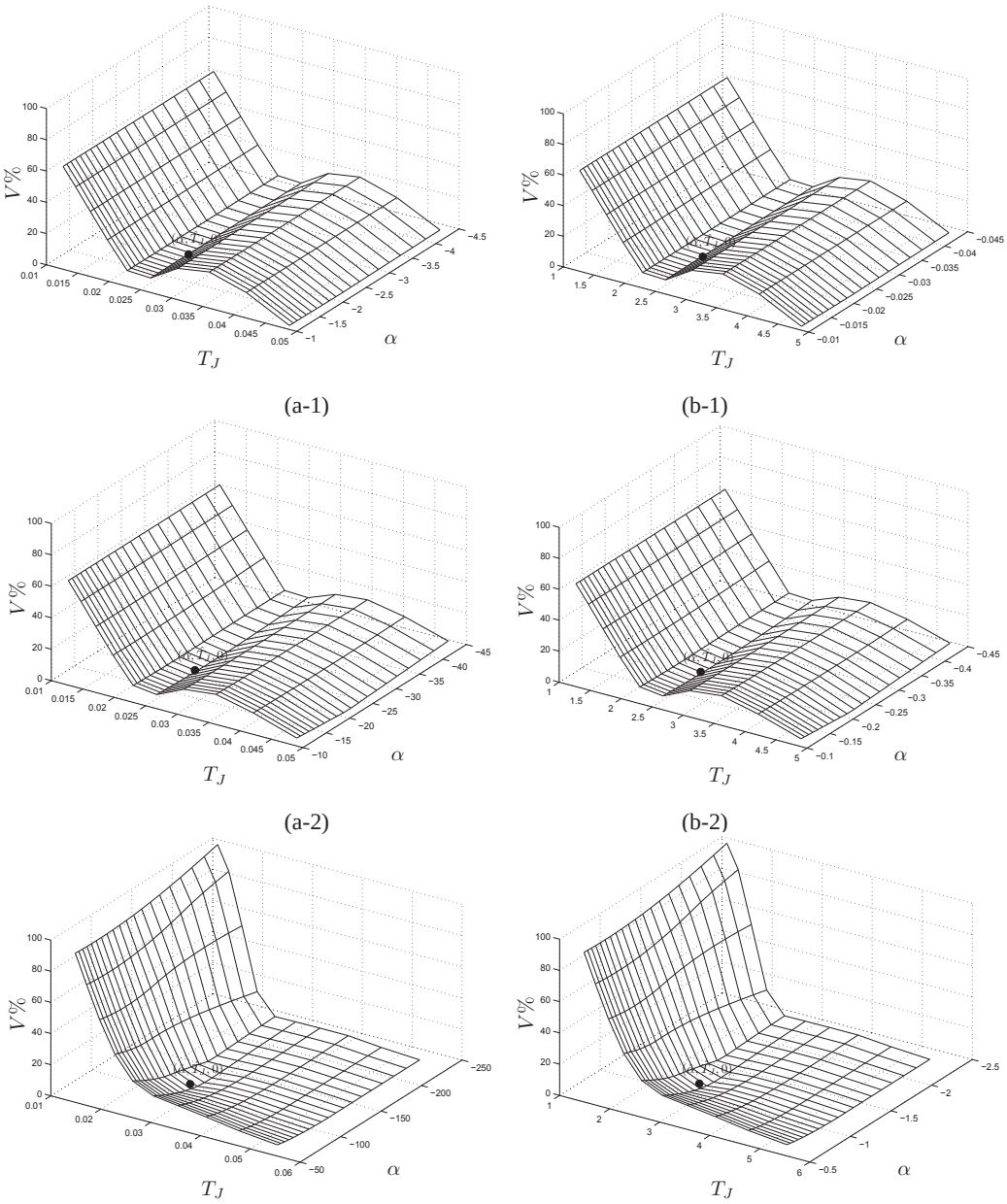

Fig. 13. Sensitivity of $F_J(s)$ to changes in σ and T_J for different values of δ and ω_n of the plant: $\delta = 0.0083$ (1), $\delta = 0.083$ (2) and $\delta = 0.45$ (3); $\omega_n = 260.53$ rad/s (a) and $\omega_n = 2.6053$ rad/s (b).

it is possible to show that the properties of $F_J(s)$ remain unaltered. As a matter of fact, because of the linearity the response of the system (11) to a filtered step input is

$$Q_l(s) = G(s)\, F_J(s) \frac{1}{s} = \Delta G(s) \left(G_{ml}(s)\, F_J(s) \frac{1}{s} \right).$$

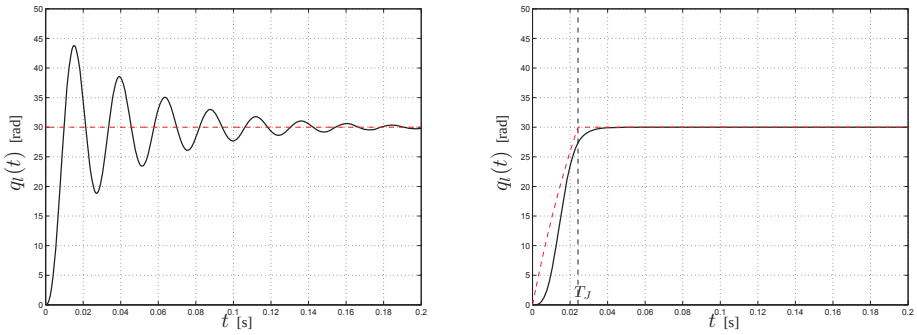

(a) (b)

Fig. 14. Response of a resonant system with an additional real pole, $G(s) = G_{ml}(s)\frac{1}{\tau s+1}$ with $\omega_n = 260.43$ rad/s, $\delta = 0.083$ and $\tau = 0.0046$s, forced by a step input of amplitude $h = 30$ rad (a) and a step input filtered by the filter $F_J(s)$ (b).

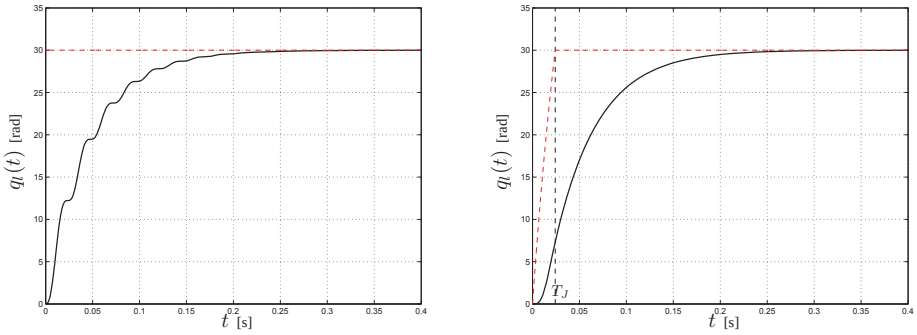

(a) (b)

Fig. 15. Response of a resonant system with an additional real pole, $G(s) = G_{ml}(s)\frac{1}{\tau s+1}$ with $\omega_n = 260.43$ rad/s, $\delta = 0.083$ and $\tau = 0.046$s, forced by a step input of amplitude $h = 30$ rad (a) and a step input filtered by the filter $F_J(s)$ (b).

Therefore, the ideal response obtained with the nominal model $G_{ml}(s)$ which, according to Theorem 1, does not have residual vibration, is simply filtered by $\Delta G(s)$. Note that the dynamics $\Delta G(s)$ will introduce additional modes in the response but cannot excite again the resonant mode of $G_{ml}(s)$ damped by the filter $F_J(s)$.

In particular, if $\Delta G(s)$ represents a dynamics faster than the nominal model $G_{ml}(s)$ and completely damped, for instance a real pole with time-constant $\tau = \frac{1}{10}\frac{1}{\delta\omega_n}$, the response of the system to a step input without and with the filter $F_J(s)$ is the one shown in Fig. 14: the presence of the additional pole involves an increased duration of the response that in the nominal case reaches the steady-state condition in T_J seconds, but the residual vibration is completely suppressed.

Even if the convergency rate of the additional pole is comparable with the rate of the undamped (complex) poles that characterize $G_{ml}(s)$ the result is similar, that is the use of $F_J(s)$ cancels the oscillations that otherwise would affect the response. See Fig. 15 where the unmodeled dynamics $\Delta G(s) = \frac{1}{\tau s+1}$ with $\tau = \frac{1}{\delta\omega_n}$ has been considered.

In case of systems with multiple vibratory modes, a single filter $F_J(s)$ is only able to cancel the oscillation due

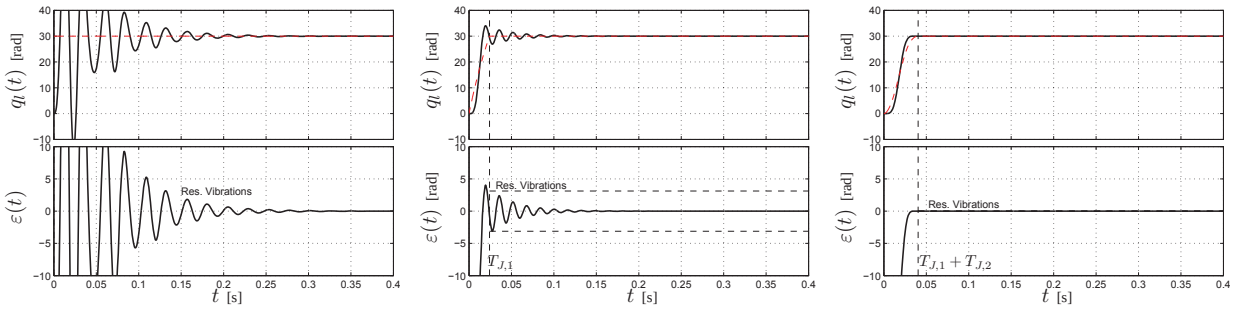

(a) (b) (c)

Fig. 16. Response of a resonant system with 2 vibrational modes characterized by $\omega_{n,1} = 260.43$ rad/s, $\omega_{n,2} = 390.6450$ rad/s and $\delta = 0.083$ forced by a step input of amplitude $h = 30$ rad (a), a step input filtered by the filter $F_J(s)$ designed to take into account ω_1 (b) and a step input filtered by two filters $F_J(s)$ which consider both ω_1 and ω_2 (c).

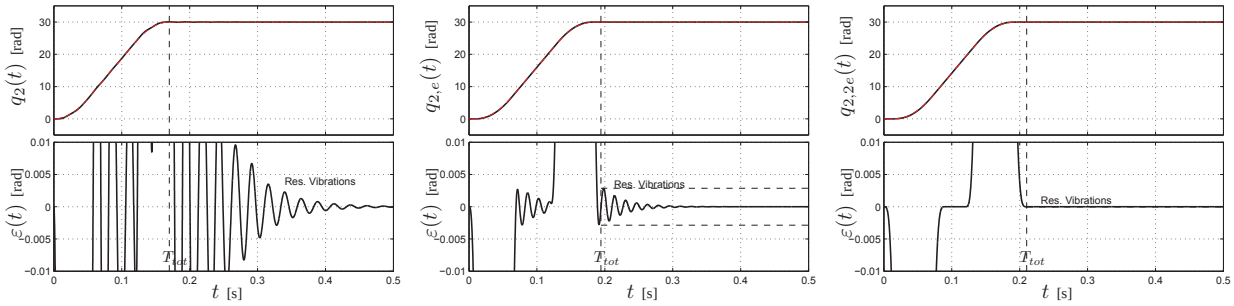

(a) (b) (c)

Fig. 17. Response of a resonant system with 2 vibrational modes characterized by $\omega_{n,1} = 260.43$ rad/s, $\omega_{n,2} = 390.6450$ rad/s and $\delta = 0.083$ forced by a second order trajectory $q_2(t)$ with $h = 30$ rad, $\mathrm{v}_{max} = 250$ rad/s, $\mathrm{a}_{max} = 5000$ rad/s^2 (a), an exponential jerk trajectory $q_{2,e}(t)$ taking into account ω_1 (b) and the trajectory $q_{2,2e}(t)$ of Fig. 18 which considers both ω_1 and ω_2 (c).

to a specific mode. As a consequence, the use of a filter $F_J(s)$ does not guarantee the complete residual vibration suppression but it is necessary to consider the cascade of two or more filters, each one related to a specific mode. In Fig. 16 the step response of a plant characterized by two modes with the same damping coefficient δ but different natural frequencies $\omega_{n,1}$ and $\omega_{n,2}$, with $\omega_{n,2} = 1.5\omega_{n,1}$ without and with filtering action is shown. A single filter $F_{J,1}(s)$ considerably reduces residual vibration but does not cancel all the oscillations. Therefore, a second filter $F_{J,2}(s)$ is necessary to completely suppress undesired vibrations with the consequent increase of the delay caused by the filters. If the two filters are not applied to a step signal but to a second order trajectory $q_2(t)$, like in Fig. 17, the capability of suppressing residual vibrations can be merged with the compliance to kinematic constraints but in this case the final trajectory is not characterized by a jerk profile composed by tracts of exponential function, see Fig. 18.

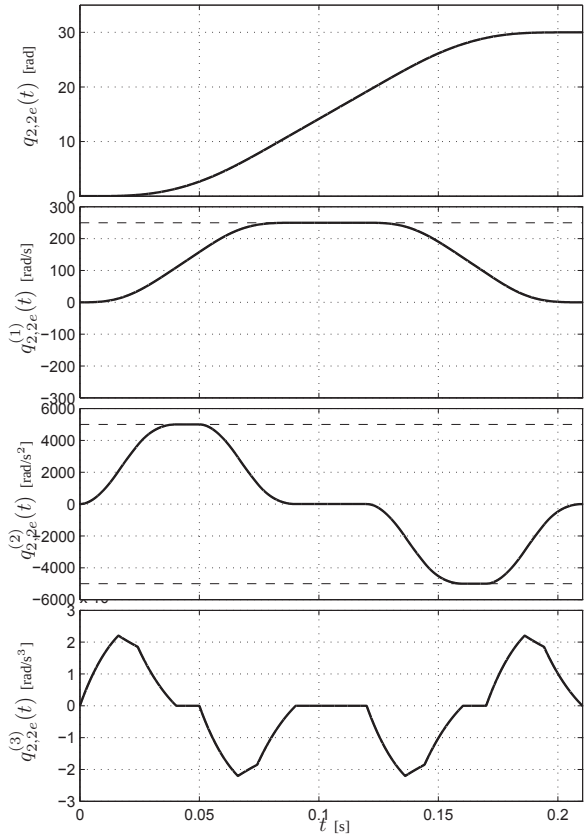

Fig. 18. Profiles of the trajectory $q_{2,2e}(t)$ obtained by applying to the trajectory $q_2(t)$ of Fig. 9(a) two exponential filters with $\omega_{n,1} = 260.43$ rad/s, $\omega_{n,2} = 389.2971$ rad/s and $\delta = 0.083$ (b).

C. Digital implementation of the trajectory filter

Since the generation of exponential jerk trajectories is based on the dynamic filters fed by step functions, i.e.

$$Q_{2e}(s) = M_1(s) \cdot M_2(s) \cdot F_J(s) \cdot \frac{h}{s}$$

it can be easily performed online by modifying the input signal. However, the practical use of the proposed filter requires its transformation in the discrete time domain (T_s denotes the sampling period) because trajectory planning is generally performed by digital controllers. This conversion can be obtained with two main techniques, being the impulse response of $F_J(s)$ of finite length:

1) it is possible to obtain the coefficients of a FIR filter by sampling the impulse response $f_J(t)$ with period T_s;
2) it is possible to deduce the IIR transfer function corresponding to $F_J(s)$ by means of usual discretization techniques.

In order to obtain a closed form expression of $F_J(z)$ the second approach has been preferred. By Z-transforming the filter $F_J(s)$ given in (6) and imposing a unitary static gain, the following expression descends

$$F_J(z) = \frac{1 - e^{\alpha\, T_s}}{1 - e^{\alpha\, T_s}\, e^{\alpha\, N_J}} \frac{1 - e^{\alpha\, T_s}\, e^{\alpha\, N_J}\, z^{-N_J}}{1 - e^{\alpha\, T_s}\, z^{-1}} \tag{12}$$

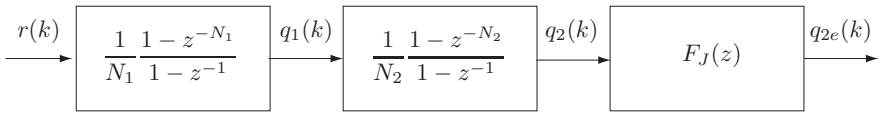

Fig. 19. Structure of the discrete-time filter for exponential jerk generation.

where $N_J = \text{round}(T_J/T_s)$. In Fig. 19 the complete structure of the discrete-time filter for online generating exponential jerk trajectories is shown. Note that in order to guarantee that the sequence $q_{2e}(k)$ of values of the discrete time-trajectory coincides with the continuous-time profile $q_{2e}(t)$ at sampling times, its expression should be obtained by Z-transforming the overall chain of continuous filters with a step input, i.e. $Q_{2e}(z) = \mathcal{Z}\{Q_{2e}(s)\}$. Therefore, the following expression can be deduced

$$Q_{2e}(z) = \frac{h}{1-z^{-1}} \cdot M_1(z) \cdot M_2(z) \cdot F_J(z) \cdot F'(z) \tag{13}$$

where $F'(z)$ is a FIR filter with unitary static gain, whose expression is

$$F'(z) = f_0\, z^{-1} + f_1\, z^{-2} + f_2\, z^{-3} \tag{14}$$

being

$$f_0 = \frac{-2 + 2e^{\rho} - 2\rho - \rho^2}{2(e^{\rho}-1)\rho^2}$$
$$f_1 = \frac{4 - 4e^{\rho} + 2\rho + 2\rho e^{\rho} - \rho^2 + \rho^2 e^{\rho}}{2(e^{\rho}-1)\rho^2}$$
$$f_2 = \frac{-2 + 2e^{\rho} - 2\rho e^{\rho} + \rho^2 e^{\rho}}{2(e^{\rho}-1)\rho^2}$$

and $\rho = \alpha T_s$. By comparing (13) with the discrete-time generator of Fig. 19, it comes out that the difference between the two output sequences is only caused by the filter $F'(z)$, whose main effect consists in a time delay of two sampling intervals[3]. By neglecting this filter, a time anticipation is therefore introduced in the generator, as shown in Fig. 20, where the step response of the continuous-time filter and the sequences obtained with the exact discretization and with the approximated generator of Fig. 19 are reported. In order to emphasize the approximation error the sampling period has been intentionally assumed very large ($T_s = 0.1$ s). In this way it is possible to appreciate that, besides the time anticipation, the discrete-time filter provides an excellent approximation of the desired trajectory. Obviously, when the sampling period decreases, the difference between $q_{2e}(t)$ and the approximated $q_{2e}(k)$ tends to vanish.

A last remark concerns the computation complexity of the proposed trajectory generator. As illustrated in Tab. II, where the difference equations of the trajectory generator of Fig. 19 are reported, at each sampling time the

[3]Since the sampling frequency ω_s is generally chosen by assuming that $\omega_s \geq 10\omega_n$, the parameter $\rho = -\delta\omega_n \frac{2\pi}{\omega_s}$ results quite small in magnitude, i.e. $-0.6283 \leq \rho \leq 0$. As a consequence, the range of variation of the coefficients defining $F'(z)$ is rather limited ($0.1412 \leq f_0 \leq 0.1667$, $0.6666 \leq f_1 \leq 0.6656$, $0.1667 \leq f_2 \leq 0.1932$). Moreover, f_1 is considerably higher than other coefficients and therefore a rough approximations of $F'(z)$ can be obtained by neglecting f_0 and f_2, and assuming that that $F'(z) \approx z^{-2}$.

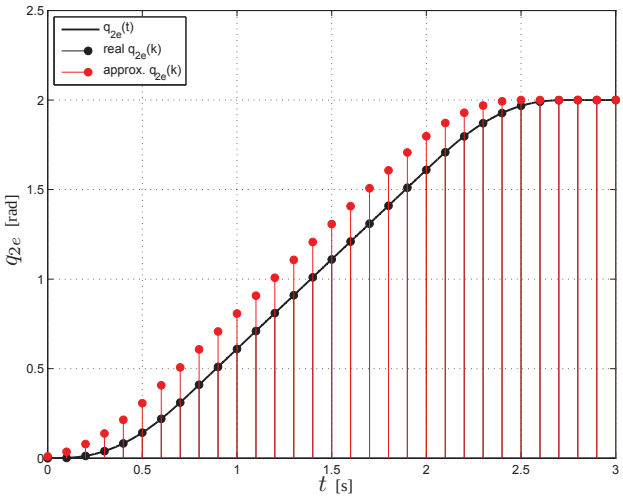

Fig. 20. Comparison between the trajectories produced by exponential jerk trajectory filters defined in the continuous- and discrete-time domain with $T_1 = 1\,\text{s}$, $T_2 = 0.6\,\text{s}$ ($N_i = \text{ceil}(T_i/Ts)$), $T_J = 0.2\,\text{s}$ and $\alpha = -3$.

$$q_1(k) = q_1(k) + a_1\Big(r(k) - r(k - N_1)\Big)$$
$$q_2(k) = q_2(k) + a_2\Big(q_1(k) - q_1(k - N_2)\Big)$$
$$q_{2e}(k) = a_3\, q_{2e}(k) + a_4\Big(q_2(k) - a_5\, q_2(k - N_J)\Big)$$

TABLE II

DIFFERENCE EQUATIONS CORRESPONDING TO THE TRAJECTORY GENERATOR OF FIG. 19 (THE VALUES OF THE CONSTANT PARAMETERS a_i ARE $a_1 = \frac{1}{N_1}$, $a_2 = \frac{1}{N_2}$, $a_3 = e^{\alpha\, T_s}$, $a_4 = \frac{1-e^{\alpha\, T_s}}{1-e^{\alpha\, T_s}\, e^{\alpha\, N_J}}$, $a_5 = e^{\alpha\, T_s}\, e^{\alpha\, N_J}$).

computation of the output of the cascade of filters requires a total of 6 additions and 5 multiplications. If the filter $F'(z)$ is considered, 2 more additions and 3 multiplications must be performed. Moreover 3 memory areas are necessary, in order to store the last N_1 values of $q_1(k)$, the last N_2 values of $q_2(k)$ and the last N_J values of $q_{2e}(k)$. Note that the trajectory generation based on the cascade of dynamic filters is considerably more efficient than the direct calculation of the closed form equations of the trajectory reported in Appendix A, which, besides a larger number of additions and multiplications, requires 2 divisions and the computation of an exponential function depending on t.

When a reference signal $r(k)$ composed by several step functions starting at generic time instants is applied to the trajectory generator of Fig. 19, the profiles shown in Fig. 21 are obtained. If the time-instants in which a new trajectory is triggered comply with the conditions reported in [15] a complex motion profile $q_{2e}(t)$ that meets velocity and acceleration constraints and cancels residual vibrations is obtained. Note that in this case the jerk profiles is no longer composed by tracts defined by an exponential function because of overlaps between adjacent jerk impulses. However, the capability of suppressing vibrations remain unaltered, as shown in Fig. 22 where the residual vibrations obtained with a second order trajectory $q_2(k)$ and with $q_{2e}(k)$ are compared.

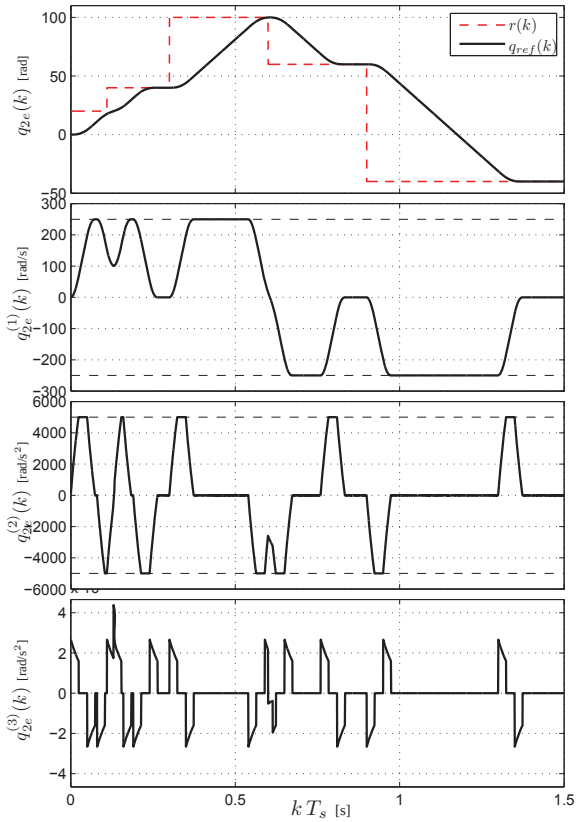

Fig. 21. Complex motion profile $q_{2e}(k)$ with $\mathrm{v}_{max} = 250$ rad/s, $\mathrm{a}_{max} = 5000$ rad/s^2, $\omega_n = 260.43$ rad/s and $\delta = 0.083$, obtained by applying to the system in Fig. 19 a reference signal $r(k)$ composed by several step functions starting at generic time instants.

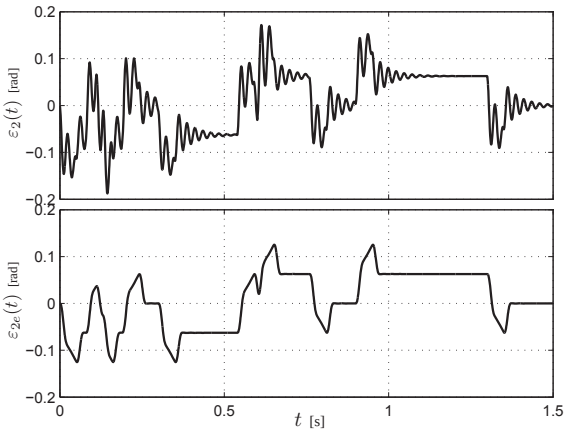

Fig. 22. Comparison between the residual vibration caused by the application to a resonant system $G_{ml}(s)$ of a second order trajectory $q_2(k)$ ($\varepsilon_2(t)$) and the corresponding exponential jerk trajectory $q_{2e}(k)$ shown in Fig. 21 ($\varepsilon_{2e}(t)$).

IV. Comparative analysis with alternative techniques for vibration suppression

As mentioned in the introduction, the main techniques for complete residual vibration suppression based on a proper filtering of the reference signal are input shaping and inversion of the plant dynamics. A first important difference between these techniques and the proposed filter $F_J(s)$ is that they do not increase the smoothness, i.e. the order of continuous derivatives, of the filtered input. They are generally applied to reference trajectories with bounded velocity and acceleration and therefore at least $\mathcal{C}^1$, that is with continuous first-order derivative, and provide as output a trajectory of the same class in case of input shapers or even of lower class if filters based on system inversion are applied. In Fig. 23 the reference signals obtained by filtering the second order trajectory $q_2(t)$ with a ZVD input shaper and with a system-inversion-based filter are shown. Note that the trajectory $q_{2,\text{zvd}}(t)$ remains $\mathcal{C}^1$, i.e. with discontinuous acceleration, and is compliant with the desired bounds imposed to the original trajectory $q_2(t)$. The trajectory $q_{2,\text{inv}}(t)$ filtered by the inverse dynamics of the plant becomes $\mathcal{C}^0$, because some discontinuities appears in the velocity profile. Moreover the bounds on the trajectory derivatives are not met anymore, see the acceleration profile of $q_{2,\text{inv}}(t)$. This behavior of the system-inversion-based filter can be rather troublesome, since as shown in Fig. 1 the system $G_{ml}(s)$ that causes vibrations only models the load and the elastic transmission of a more complex system which includes also the actuator, supposed to be able to perfectly track the reference trajectory $q_{ref}(t)$. Therefore the simplified scheme of a standard motion system with elastic linkage results as in Fig. 24. Unfortunately, any kind of actuation system is characterized by physical limitations on velocity and acceleration and if these bounds are not met the trajectory becomes unfeasible. Moreover, the requirement of perfect tracking relates the smoothness of the reference trajectory, supposed $\mathcal{C}^p$, with the relative degree r of the linear time-invariant system describing the actuation system [4], i.e

$$p \geq r - 1.$$

As a consequence, in case of an electric actuator, with $r = 3$, the reference position for the motor[4] must be at least $\mathcal{C}^2$. This implies that if an input shaping filter is used for vibrations suppression, the second order trajectory $q_2(t)$ is not sufficient but a $\mathcal{C}^2$ function is required. With an inverse dynamics filter a $\mathcal{C}^3$ trajectory must be used. Conversely, the proposed filter $F_J(s)$, that increases the smoothness of the input trajectory, needs a simple $\mathcal{C}^1$ function, like the

[4]Note that the transfer function of a standard DC motor is

$$G_a(s) = \frac{Q_m(s)}{V(s)} = \frac{K_i}{L_a J_m s^3 + (R_a J_m + B_m L_a)s^2 + (K_b K_i + R_a B_m)s}$$

where K_i is the torque constant, K_b the back-emf constant, R_a the armature resistance, L_a the armature inductance, J_m the rotor inertia, B_m the viscous-friction coefficient and $V(s)$ denotes the Laplace transform of the input voltage [5]. A feed-forward control that in nominal case assures perfect tracking is

$$V_{ff}(s) = G_a^{-1}(s)Q_{ref}(s) = \left(\frac{L_a J_m}{K_i}s^3 + \frac{R_a J_m + B_m L_a}{K_i}s^2 + \frac{K_b K_i + R_a B_m}{K_i}s\right) Q_{ref}(s)$$

which corresponds to

$$v_{ff}(t) = \frac{L_a J_m}{K_i} q_{ref}^{(3)}(t) + \frac{R_a J_m + B_m L_a}{K_i} q_{ref}^{(2)}(t) + \frac{K_b K_i + R_a B_m}{K_i} q_{ref}^{(1)}(t).$$

The control action $v_{ff}(t)$ is feasible, that is $v_{ff}(t) < \infty$, only if $q_{ref}^{(3)}(t)$ is limited and accordingly the reference trajectory $q_{ref}(t) \in \mathcal{C}^2$.

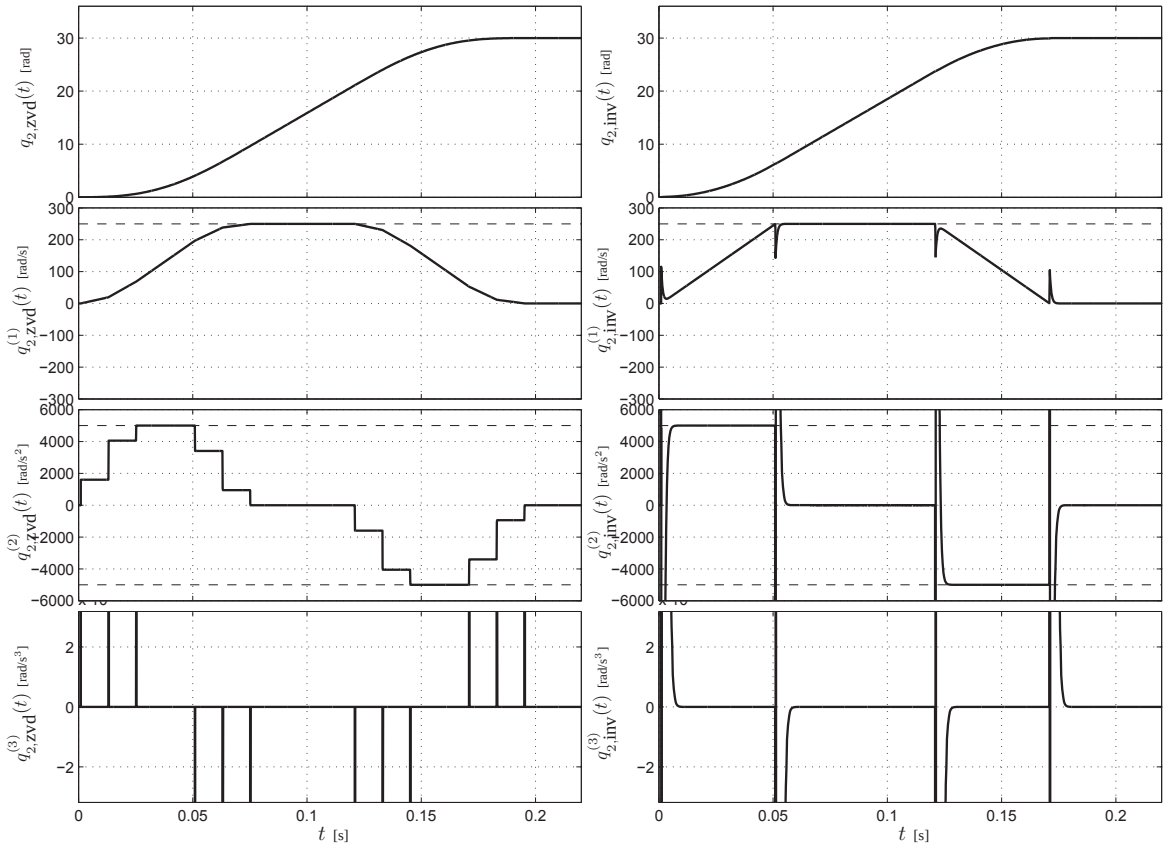

(a) (b)

Fig. 23. Reference signals obtained by filtering the second order trajectory $q_2(t)$ of Fig. 9(a) with a ZVD input shaper (a) and with the inverse dynamics of the plant (b).

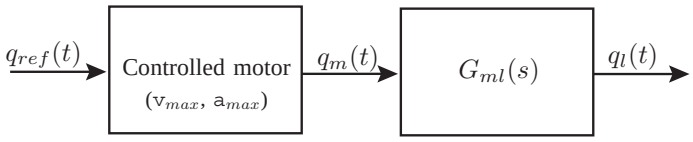

Fig. 24. Complete model of a motion system with elastic linkage.

function $q_2(t)$ which leads to the exponential jerk trajectory of Fig. 9.

From a functional point of view, input shapers, system-inversion-based filter and the proposed filter $F_J(s)$ guarantee the complete vibration suppression in nominal conditions. However, since all these techniques rely on a precise modeling of the plant, it is necessary to evaluate their robustness with respect to errors in model parameters, i.e. δ and ω_n in (3). To this aim, the different approaches have been evaluated by considering the percent residual vibration of system (3) as a function of the errors in the estimation of its parameters. Since the inverse-dynamics filter requires a continuous input function, the comparative analysis has been conducted by using the trajectory $q_2(t)$ as test function in lieu of the standard step signal. By means of extensive simulations, the curves reported in

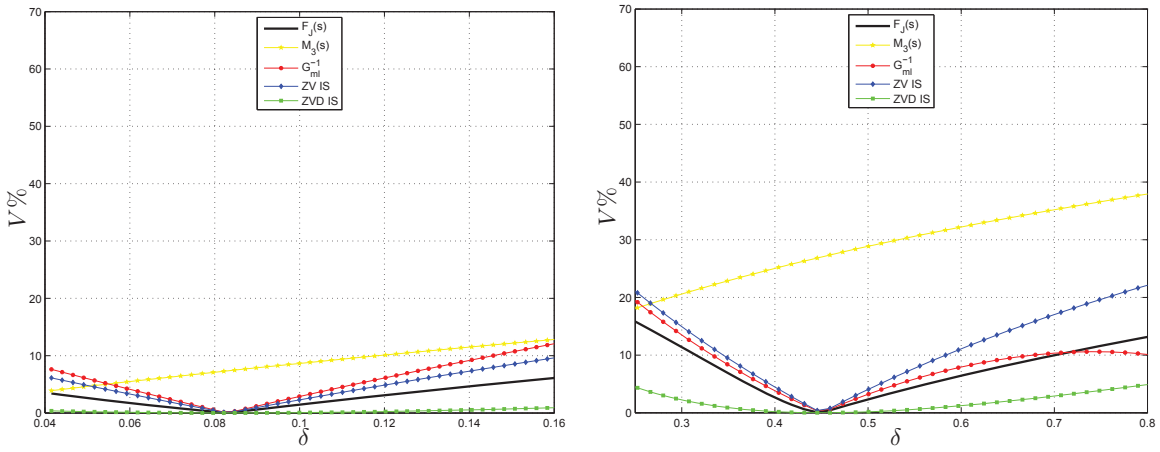

(a) (b)

Fig. 25. Percent residual vibration as a function of the damping coefficient δ about the nominal value $\hat{\delta} = 0.081$ (a) and $\hat{\delta} = 0.45$ (b).

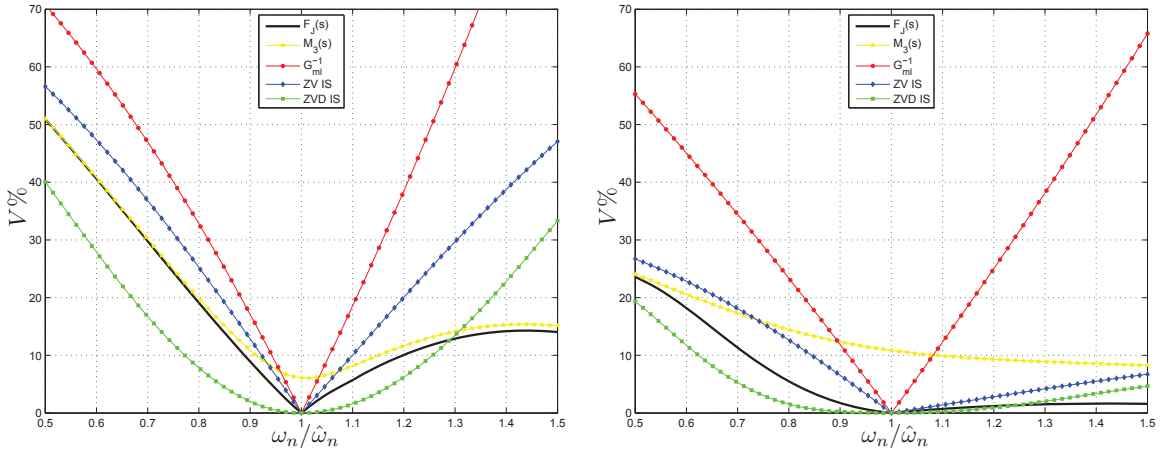

(a) (b)

Fig. 26. Percent residual vibration as a function of the ratio $\omega_n/\hat{\omega}_n$, where ω_n is the actual natural frequency of $G_{lm}(s)$ and $\hat{\omega}_n$ is the nominal value used to define the filter, for $\delta = 0.081$ (a) and $\delta = 0.45$ (b).

Fig. 25 and Fig. 26 have been obtained. For the sake of clarity, the variations of parameters δ and ω_n with respect to their nominal values are considered separately. In Fig. 25 the percent residual vibration is shown as a function of δ. Since the nominal value $\hat{\delta}$ influences the results, two different values have been considered in order to show the behavior of the different filters for small and large damping coefficients ($\hat{\delta} = 0.081$ and $\hat{\delta} = 0.45$ respectively). For the natural frequency, the nominal value $\hat{\omega}_n = 260.53$ rad/s has been assumed, but it is worth noticing that the percent residual vibration does not depends on this particular value.

The relationship between actual value of natural frequency and percent residual vibration is shown in Fig. 26, where the ratio $\omega_n/\hat{\omega}_n$ has been considered. Also in this case two different values of δ have been taken into account.

These curves highlight that for all the filters the value of the natural frequency is significantly more critical than

the damping coefficient. The proposed filter $F_J(s)$ is characterized by an intermediate robustness between ZV and ZVD input shapers, and results much more robust than system-inversion-based filters. Moreover, for high values of ω_n, $F_J(s)$ offers the best performances, see Fig. 26. The filter $M_3(s)$, that produces constant jerk trajectories, provides similar results for small values of δ (see Fig. 26(a)), but cannot reduce residual vibrations when the damping coefficient is significantly different from zero.

Finally, a fair comparison between these methods requires also an estimation of the time-delay that the filters introduce and of the consequent increase of the motion duration. With this respect, it is well-known that an higher robustness of Input Shapers is obtained by increasing the number of impulses that form the shapers and accordingly the delay introduced in the motion generation.

System-inversion-based filters do not cause any delay in the reference signal tracking. However, the need for smoother trajectories implies higher durations of the motion with respect to lower order trajectories, the bounds on velocity, acceleration, and higher derivatives being equal. Input shapers, like ZV and ZVD filters, introduce in the system time-delays similar to that caused by the $F_J(s)$ filter; in particular the additional delays are $T_J/2$ for ZV and T_J for ZVD, but also in this case the need for higher order input trajectories with respect to the filter $F_J(s)$ may increase the total duration of the motion.

V. Experimental validation

In order to experimentally test the proposed method the setup of Fig. 27 has been arranged. This simple system is characterized by a linear motion but the dynamic model described in Sec. II remains valid. It is composed by a linear motor, LinMot PS01-37x120, whose slider is connected to an inertial load by means an elastic transmission obtained with a coil spring. The load is placed on a linear guide in order to guarantee the axial alignment with the motor slider and to reduce static friction. The control system is based on the servo controller LinMot E2010-VF that performs the basic current control, while the position control (based on a PID controller and a feedforward action) has been implemented on a standard PC with a Pentium IV 3 GHz processor and 1 GB of RAM, equipped with a Sensoray 626 data acquisition board, used to both communicate with the servo controller and acquire the sensors signals. The position of the motor is measured by an incremental encoder with a resolution of $1\mu m$ integrated in the stator, and the monitoring of vibrations is obtained via a load cell connected between the slider and the elastic transmission. As a matter of fact, the force f_k exerted by the spring is proportional to the error ε between motor position and load position, and, if the inherent damping of the transmission is considered, like in Fig. 1, force f_k is simply a scaled, low-pass filtered version of ε.

The real-time operating system RTAI-Linux on a Debian SID distribution with Linux kernel 2.6.17.11 and RTAI 3.4 allows the position controller to run with a sampling period $T_s = 500\mu s$. For the design of the control scheme and of trajectory generator, the MatLab/Simulink/RealTime Workshop environment has been used.

In Tab. III the main characteristics[5] of the mechanical system are reported. The value of the internal damping b_t

[5]The symbols refer to the model of Fig. 1(b).

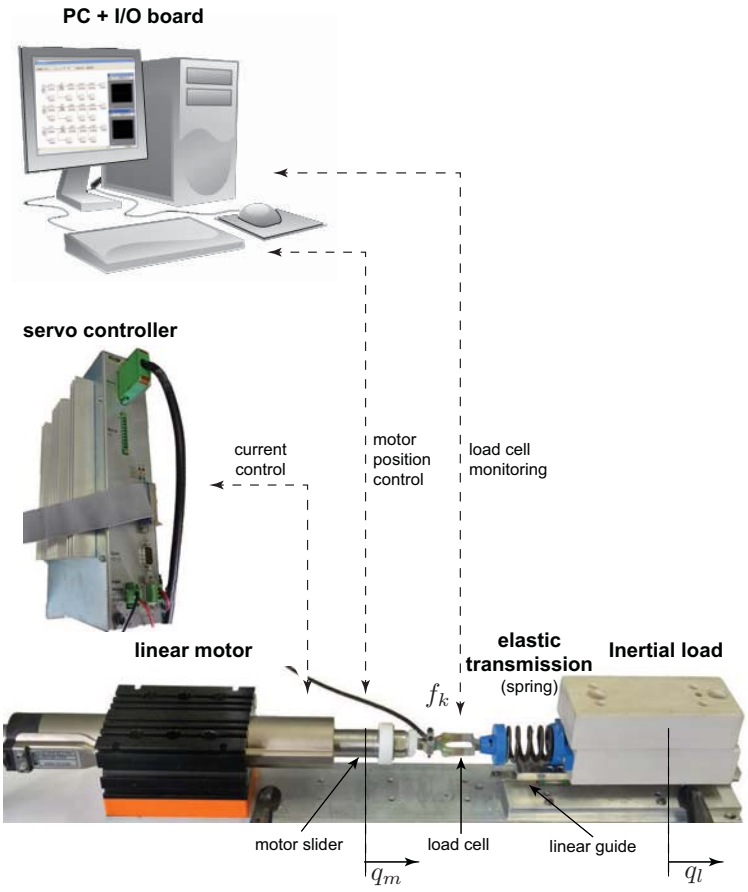

Fig. 27. Experimental setup.

Parameter	Symbol	Value	Unit
Slider mass	J_m	0.599	kg
Load mass	J_l	0.623	kg
Spring stiffness	k_t	6490	N m

TABLE III

MOTION SYSTEM PARAMETERS.

is unknown, but it can be easily deduced from the parameters α and T_J of the filter $F_J(s)$. The value of these parameters is obtained as described in Sec. III-A but the oscillation is induced by physically blocking the motor slider and applying an initial deformation to the spring. In Fig. 28, the force $f_k(t)$ recorded during an experiment is shown together with the force of the identified system characterized by $\hat{\delta} = 0.0246$ and $\hat{\omega}_n = 101.3724$ rad/s, which correspond to $\hat{\alpha} = -2.4958$ and $\hat{T}_J = 0.0620$ s (indeed, several tests have been performed and the mean value of the parameters has been assumed). Note that the value of ω_n found in the experiments is consistent with the theoretical value $\sqrt{k_t/J_l} = 102.0653$ rad/s. The main difference between the responses of real and ideal

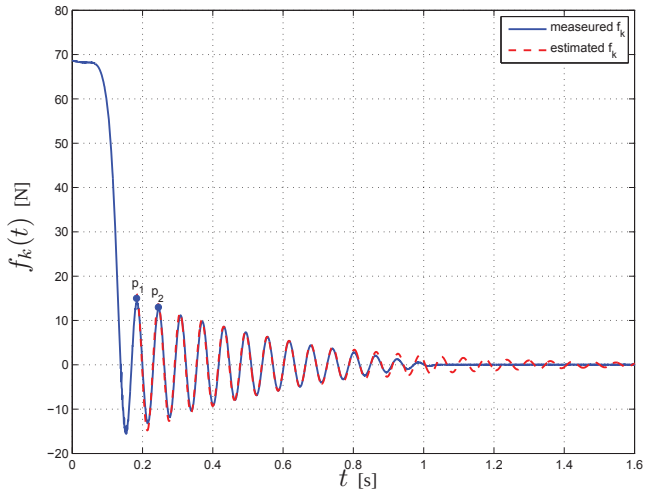

Fig. 28. Oscillations of the system of Fig. 27 used for the identification of the parameters of filter $F_J(s)$.

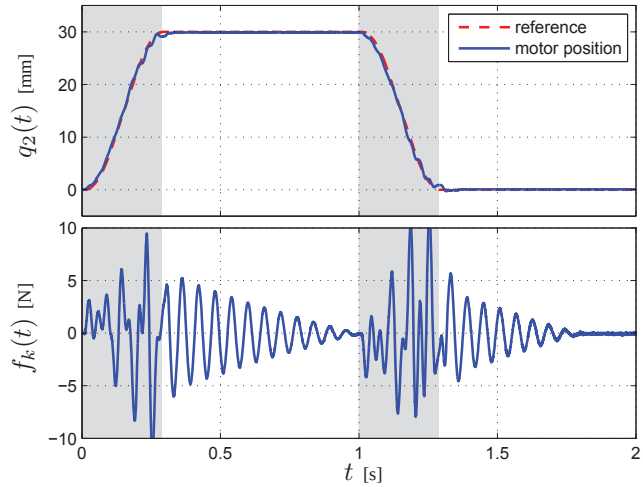

Fig. 29. Residual vibrations induced in the system of Fig. 27 by the application of a second order trajectory $q_2(t)$.

system lies in the manner in which the oscillation vanishes, see Fig. 28 for $t \geq 0.9$ s: the model's output goes to zero asymptotically while the real system suddenly stops probably because of the (unmodeled) static friction. Moreover, besides the vibratory dynamics $G_{ml}(s)$ the model of the real system should include the poles of the controlled actuator, but since the control feedback has been designed with a very high bandwidth these poles have been neglected. As a matter of fact, as already noted in Sec. III-B unmodeled poles faster than the mechanical dynamics that induces vibrations do not modify significantly the results of the application of the filter $F_J(s)$ and of the exponential jerk trajectories.

In Fig. 29, the response of the system to second-order trajectory $q_2(t)$ used as basic motion profiles is reported. This trajectory, characterized by a total displacement h of 30 mm, has been obtained by means of the first two

filters in Fig. 19 with $N_i = T_i/T_s$, $i = 1, 2$, being $T_2 = 1.5\,\hat{T}_J = 0.0930\,\text{s}$ and $T_1 = 2\,T_2 = 0.1860\,\text{s}$. With these parameters, the maximum velocity and the maximum acceleration are $\mathtt{v}_{max} = 0.1613\,\text{m/s}$ and $\mathtt{a}_{max} = 1.7343\,\text{m/s}^2$ respectively. Obviously the behavior of the system at the end of motion (highlighted in the plots with the white background) is very similar to that of the uncontrolled system of Fig. 28.

When the filter $F_J(z)$ is added and the exponential jerk trajectory is applied to the resonant system, the residual vibration is considerably reduced, see Fig. 30(a). However, it is not completely cancelled. Note that the residual vibration seems not due to additional unmodelled (linear) dynamics of the plant since its period is exactly $\hat{T}_J$. Instead, the cause must be probably sought in nonlinear phenomena (i.e. the static and Coulomb friction on the motor slider) and external disturbances (such as the cogging which is present in the linear motor) affecting the system. These effects are probably not completely compensated by the motor controller and the actuator does not behave like an ideal position source.

In order to evaluate the benefits of the proposed method in real applications, its behavior has been compared with those of the alternative approaches mentioned in Sec. IV, which should lead to a complete cancellation of residual vibrations. In particular, in Fig. 30(b) the response of the experimental setup to the trajectory $q_2(t)$ filtered by a ZVD input shaper is shown, and in Fig. 30(c) the result with the inverse dynamics filter is reported. The actual capabilities of the exponential jerk trajectory and of the input shaper in vibrations suppression are comparable, while the filter based on the dynamics inversion shows a lower robustness with respect to the above mentioned non-idealities: the level of vibrations decreases with respect to those obtained with the direct application of $q_2(t)$ only for a positive displacement of the motor, while it remains practically unchanged if the motion occurs along the negative direction[6].

Note that the vibrations reduction shown in Fig. 30 with respect to Fig. 29 is marginally caused by the increase of the time-duration of the trajectory because of the additional filters. As a matter of fact, both for the exponential jerk trajectory and for the trajectory filtered by the input shaper the duration of the motion is $T_{tot} = T_1 + T_2 + \hat{T}_J = 0.3410\,\text{s}$. Therefore, in order to perform a more precise comparison, a second-order trajectory $q_2(t)$ with the same total duration (that is $T_2 = 0.1137\,\text{s}$ $T_1 = 2\,T_2$ and $T_{tot} = T_1 + T_2 = 0.3410\,\text{s}$) has been applied to the mechanical system. The result, illustrated in Fig. 31, confirms that the reduction of the residual vibration obtained with a simple time-scaling is rather limited if compared with the proposed approach, the overall duration of the motions being equal.

Finally, the robustness of the filter F_J with respect to errors in the parameter T_J has been experimentally tested. In Fig. 32(a) and Fig. 32(b) the responses of the system to the exponential jerk trajectory computed with the parameter T_J equal to $0.5\hat{T}_J$ and $1.5\hat{T}_J$ are reported, and confirm that an underestimation of T_J makes the filter F_J less effective while an overestimation of T_J lead to small residual vibrations. Conversely, with ZVD input shapers only the nominal values of the parameters produce good performances. In fact, both underestimation and overestimation of T_J cause large residual vibrations, see Fig. 32(c) and (d). Note that in the test reported in Fig. 32(b) the residual

[6]Several tests have been performed but the result was always the same

vibration is even smaller than the vibration obtained with the nominal value of parameter T_J and shown in Fig. 30(a). This is probably due to the fact that the higher duration of the trajectory, i.e. $T_{tot} = T_1 + T_2 + 1.5\hat{T}_J = 0.3808\,\text{s}$, with respect to the nominal trajectory, for which $T_{tot} = 0.3410\,\text{s}$, mitigates the above mentioned non-ideal phenomena, like friction and cogging, and allows the motor to better track the given profile $q_{ref}(t)$.

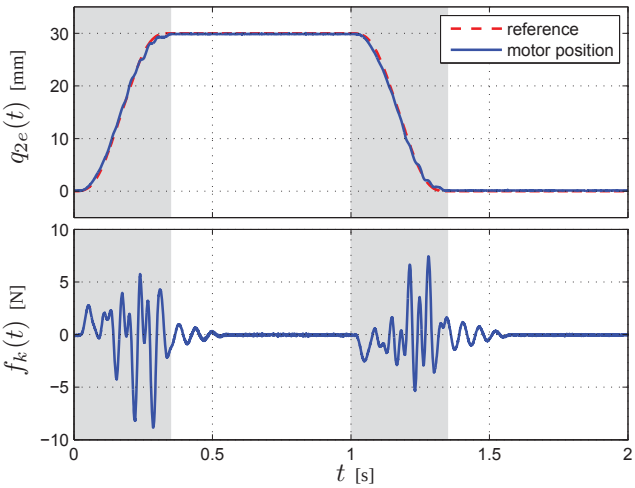

(a)

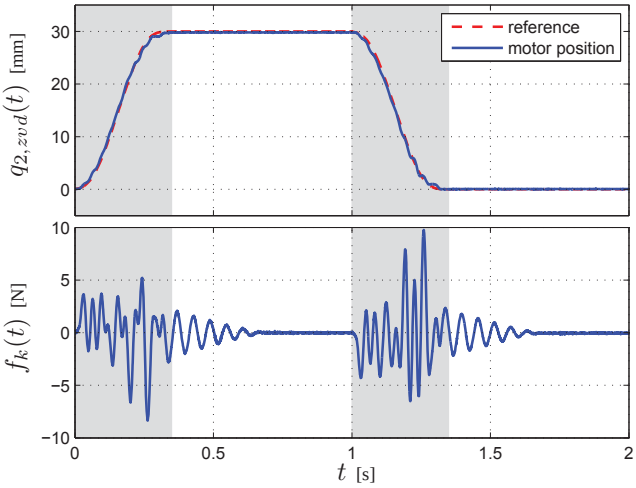

(b)

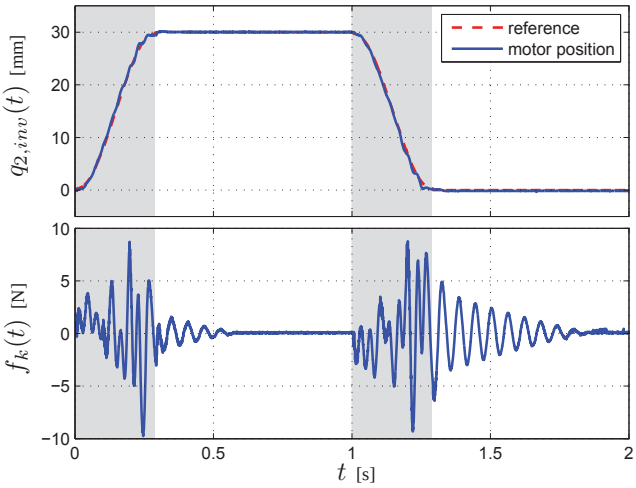

(c)

Fig. 30. Comparison between residual vibrations induced in the system of Fig. 27 by the application of an exponential jerk trajectory (a), a second order trajectory filtered by a ZVD input shaper (b) and a second order trajectory filtered by the system inverse dynamics (c).

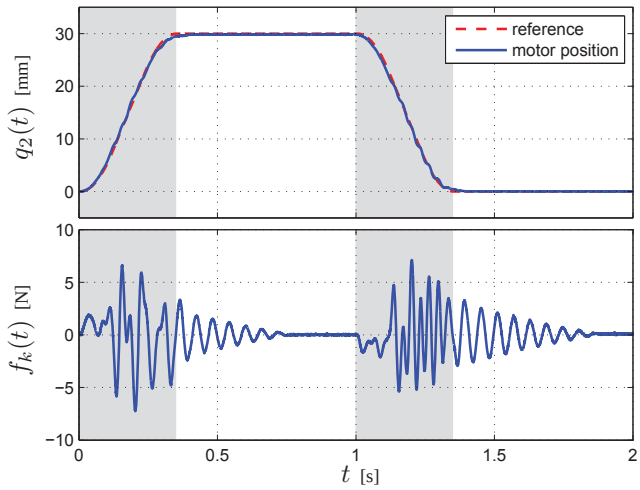

Fig. 31. Residual vibrations induced in the system of Fig. 27 by the application of a second order trajectory $q_2(t)$ with $T_2 = 0.1137$s.

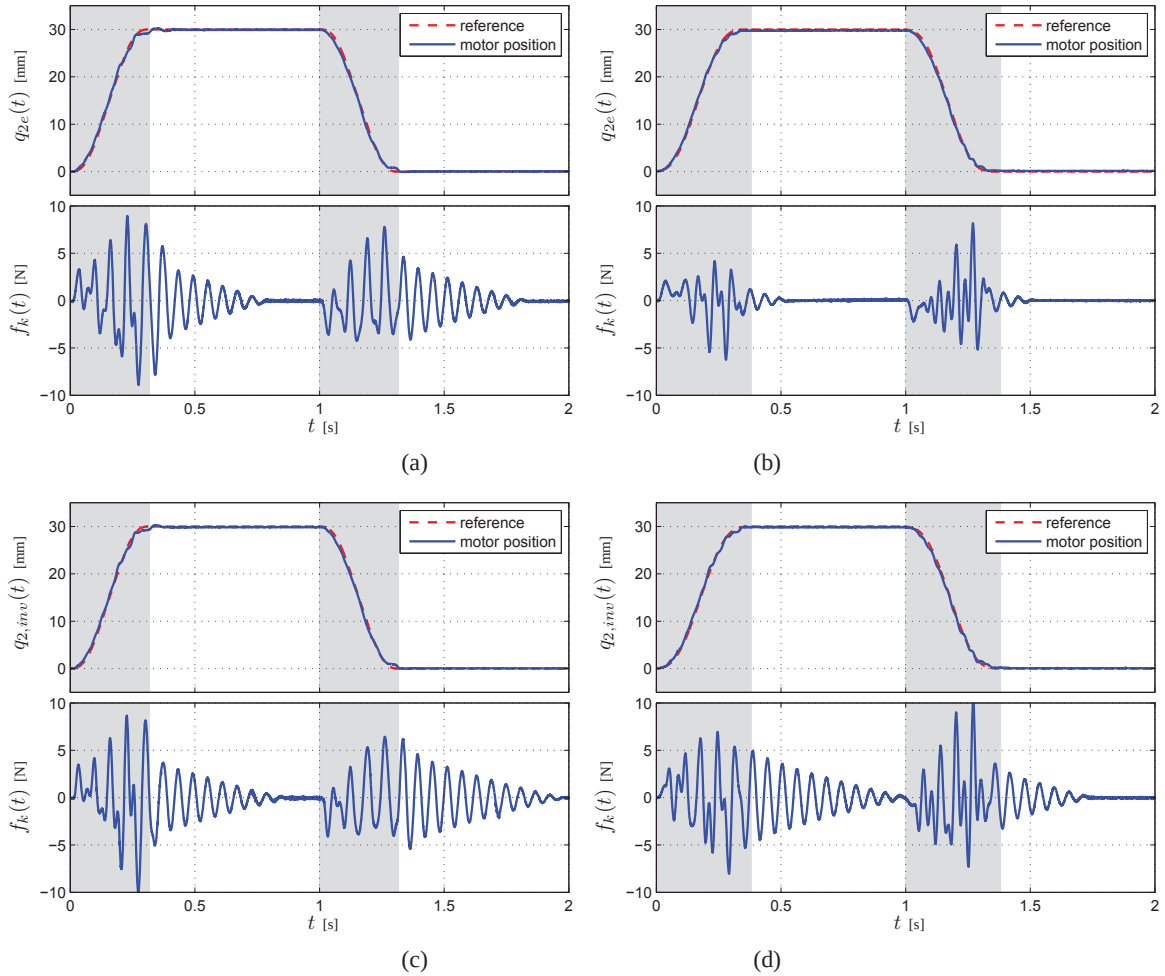

Fig. 32. Residual vibrations induced in the system of Fig. by an exponential jerk trajectory with $T_J = 0.5\hat{T}_J$ (a) and $T_J = 1.5\hat{T}_J$ (b), and by a second order trajectory filtered by a ZVD input shaper with $T_J = 0.5\hat{T}_J$ (c) and $T_J = 1.5\hat{T}_J$ (d).

VI. Conclusions

The use of exponential jerk trajectories, which can be efficiently generated by filtering standard trapezoidal trajectories, allows to considerably reduce the vibrations level in motion systems with elastic transmission. Ideally, the proposed filters, characterized by the parameters α and T_J which can be easily deduced from the response of the resonant system, is able to completely cancel the residual vibration. Experimental tests have demonstrated that the proposed approach has performances similar to well-known input shaping techniques and system-inversion-based filters, but compared to these methods it guarantees a superior robustness with respect to errors in the parameters estimation. Moreover, this technique offers considerable advantages in terms of smoothness of the motion profiles: if the input trajectory is $\mathcal{C}^p$ (e.g. $p = 1$ for trapezoidal velocity trajectories) the filtered trajectory will be $\mathcal{C}^{p+1}$ and the peak values of the first $p + 1$ derivatives of the original trajectory will not be exceeded by the new trajectory. In this way, it is possible to design exponential jerk trajectories compliant with kinematic constraints on velocity and acceleration and with vibrations cancelling capabilities.

Appendix A
Analytic expression of a seven-segment trajectory with exponential jerk

The expression of a point-to-point third order trajectory compliant with constraints on the maximum velocity $\mathtt{v}_{max}$ and acceleration $\mathtt{a}_{max}$, and with jerk impulses characterized by a duration T_J and a decay rate α is

$$q_{2,e}(t) = \begin{cases} q_1(t,\alpha), & 0 \le t < T_J \\ q_2(t,\alpha), & T_J \le t < T_2 \\ q_3(t,\alpha), & T_2 \le t < T_2 + T_J \\ q_4(t,\alpha), & T_2 + T_J \le t < T_1 \\ h - q_3(T_{tot} - t, -\alpha), & T_1 \le t < T_1 + T_J \\ h - q_2(T_{tot} - t, -\alpha), & T_1 + T_j \le t < T_1 + T_2 \\ h - q_1(T_{tot} - t, -\alpha), & T_1 + T_2 \le t \le T_{tot} \end{cases}$$

where h is the total displacement from initial point (supposed to be zero) to the final point, $T_{tot} = T_1 + T_2 + T_J$ denotes the total duration of the trajectory (which starts at $t_0 = 0$), and

$$
\begin{aligned}
q_1(t,\alpha) &= \mathtt{a}_{max}\frac{2 - 2\,e^{\alpha\,t} + \alpha\,t\,(2+\alpha\,t)}{2\,\alpha^2(1-e^{\alpha\,T_J})}\\
q_2(t,\alpha) &= \mathtt{a}_{max}\left[\frac{2+\alpha\,t(2+\alpha\,t)}{2\,\alpha^2(1-e^{\alpha\,T_J})} - \right.\\
&\qquad \left. - \frac{e^{\alpha T_J}(2+\alpha(2+\alpha(t-T_J))(t-T_J))}{2\,\alpha^2(1-e^{\alpha\,T_J})}\right]\\
q_3(t,\alpha) &= \mathtt{a}_{max}\left[\frac{2\,e^{\alpha(t-T_2)} + \alpha\,T_2\,(2\,(1+\alpha\,t) - \alpha\,T_2)}{2\,\alpha^2(1-e^{\alpha\,T_J})} - \right.\\
&\qquad \left. - \frac{e^{\alpha\,T_J}(2+2\,\alpha(t-T_J)+\alpha^2(t-T_J)^2)}{2\,\alpha^2(1-e^{\alpha\,T_J})}\right]\\
q_4(t,\alpha) &= \mathtt{v}_{max}\frac{2+2\alpha t-\alpha T_2 - e^{\alpha T_J}(2+\alpha(2t-2T_J-T_2))}{2\,\alpha(1-e^{\alpha\,T_J})}
\end{aligned}
$$

The time intervals T_1 and T_2 must be computed according to (4) with the additional conditions

$$T_1 \geq T_2 + T_J, \qquad T_2 \geq T_J$$

which guarantee that all the seven segments composing the trajectory are present.

REFERENCES

[1] P. Lambrechts, M. Boerlage, and M. Steinbuch, "Trajectory planning and feedforward design for electromechanical motion systems," *Control Engineering Practice*, vol. 13, pp. 145–157, 2005.

[2] P.-J. Barre, R. Béarée, P. Borne, and E. Dumetz, "Influence of a jerk controlled movement law on the vibratory behaviour of high-dynamics systems," *Journal of Intelligent and Robotic Systems*, vol. 42, pp. 275–293, 2005.

[3] P. Meckl and P. Arestides, "Optimized s-curve motion profiles for minimum residual vibration," in *Proceedings of the American Control Conference*, Philadelphia, Pennsylvania, 1998, pp. 2627–2631.

[4] J. S. Dewey and S. Devasia, "Experimental and theoretical results in output-trajectory redesign for flexible structures," in *Decision and Control, 1996., Proceedings of the 35th IEEE Conference on*, vol. 4, Dec 1996, pp. 4210–4215 vol.4.

[5] B. C. Kuo and F. Golnaraghi, *Automatic Control Systems*, 8th ed. New York, NY, USA: John Wiley & Sons, Inc., 2002.

[6] W. Singhose, N. Singer, and W. Seering, "Comparison of command shaping methods for reducing residual vibration," in *Third European Control Conf*, 1995, pp. 1126–1131.

[7] O. J. M. Smith, "Posicast control of damped oscillatory systems," *Proceedings of the IRE*, vol. 45, no. 9, pp. 1249–1255, Sept 1957.

[8] N. C. Singer and W. P. Seering, "Preshaping command inputs to reduce system vibration," *ASME Journal of Dynamic Systems, Measurement, and Control*, vol. 112, pp. 76–82, 1990.

[9] T. Tuttle and W. Seering, "A zero-placement technique for designing shaped inputs to suppress multiple-mode vibration," in *American Control Conference, 1994*, vol. 3, 1994, pp. 2533 – 2537.

[10] K.-T. Hong and Hong, "Input shaping and vsc of container cranes," in *Proc. IEEE International Conference on Control Applications*, 2004, pp. 1570–1575.

[11] J. Fortgang, W. Singhose, and J. d. J. Mrquez, "Command shaping for micro-mills and cnc controllers," in *Proc. American Control Conference*, 2005.

[12] D. Magee and W. Book, "Optimal filtering to minimize the elastic behavior in serial link manipulators," in *American Control Conference, 1998. Proceedings of the 1998*, vol. 5, Philadelphia, PA , USA, 1998, pp. 2637 – 2642.

[13] A. Piazzi and A. Visioli, "Minimum-time system-inversion-based motion planning for residual vibration reduction," *Mechatronics, IEEE/ASME Transactions on*, vol. 5, no. 1, pp. 12–22, Mar 2000.

[14] J. J. Kim and B. Agrawal, "Experiments on jerk-limited slew maneuvers of a flexible spacecraft," in *Guidance, Navigation, and Control and Co-located Conferences*. American Institute of Aeronautics and Astronautics, Aug. 2006, pp. –.

[15] L. Biagiotti and C. Melchiorri, "FIR filters for online trajectory planning with time- and frequency-domain specifications," *Control Engineering Practice*, vol. 20, no. 12, pp. 1385 – 1399, 2012.

[16] R. Béarée, "New damped-jerk trajectory for vibration reduction," *Control Engineering Practice*, vol. 28, no. 0, pp. 112 – 120, 2014.

[17] K. Kozak, W. Singhose, and I. Ebert-Uphoff, "Performance measures for input shaping and command generation," *Journal of Dynamic Systems Measurement and Control*, vol. 128, no. 3, pp. 731–736, 2006.